



Research article

Exponential synchronization analysis for complex dynamical networks with hybrid delays and uncertainties under given control parameters

Saravanan Shanmugam¹, Mohamed Rhaima^{2,*} and Hamza Ghoudi³

¹ Centre for Nonlinear Systems, Chennai Institute of Technology, Chennai 600 069, Tamil Nadu, India

² Department of Statistics and Operations Research, College of Sciences, King Saud University, P.O. Box 2455 Riyadh 11451, Saudi Arabia

³ University of Paris Nanterre, MODAL'X, BAT G, 200, ave de la République 92000 Nanterre, France

* **Correspondence:** Email: mrhaima.c@ksu.edu.sa.

Abstract: This paper addresses the problem of exponential synchronization in continuous-time complex dynamical networks with both time-delayed and non-delayed interactions. We employ a proportional integral derivative (PID) control strategy and a dynamic event-triggered approach to investigate this synchronization problem. Our approach begins with constructing a general model for complex dynamical networks that incorporate delays. We then derive synchronization criteria based on the PID control parameters, utilizing linear matrix inequality techniques in conjunction with a dynamic event-trigger mechanism. The application of Lyapunov stability theory and inequality techniques allows us to establish these criteria, considering the presence of hybrid delays. To illustrate the effectiveness of our proposed model, we provide two numerical examples showcasing synchronization dynamics. These examples demonstrate the successful theoretical results of a novel PID controller and dynamic event-trigger mechanism.

Keywords: complex dynamical networks; exponential synchronization; Lyapunov-Krasovskii functional; PID control

Mathematics Subject Classification: 93B20, 92D20

1. Introduction

Complex dynamical networks (CDNs) are large-scale networks comprising numerous nodes interconnected through specific topological links. CDNs with hybrid delays are crucial for modeling and optimizing real-world systems that exhibit both continuous and discrete delays. These networks

find applications in various industries, including communication networks, control systems, biological systems, power systems, economics and finance, chemical engineering, transportation, environmental sciences, mechanical systems and healthcare, such as in [1–9]. Hybrid delay models provide a robust framework for analyzing and improving the behavior of complex systems in these domains by considering the interplay between continuous dynamics and discrete events, ultimately leading to enhanced performance and efficiency. The understanding and management of complex systems, whether observed in natural phenomena or constructed systems like biological neuron networks, power grids, social connections or the Internet, have seen significant advancements in recent research, as highlighted in [10–15]. To gain deeper insights into contemporary systems, it becomes imperative to examine both the network structure and dynamic properties of complex networks.

Recent studies have extensively investigated the synchronization dynamics of CDNs composed of coupled oscillators, deriving synchronization criteria for networks with coupling delays, considering both delay-independent and delay-dependent stability of the synchronization manifold. Moreover, researchers have increasingly focused on synchronization phenomena within complex networks, serving as a framework for understanding various phenomena. Synchronization occurs when the discrepancy between driving and responding vectors approaches zero in norm. Furthermore, the concept of stability, as explored in works such as [16–22], also provides insights into the idea of synchronization.

Achieving synchronization among CDN nodes is a complex challenge influenced by architectural intricacies, network topology, environmental factors, and connectivity efficiency. Control mechanisms play a pivotal role in enabling engineering system designers to achieve impressive performance by seamlessly adapting to varying environmental conditions. This adaptability is crucial for engineering systems to function effectively and reliably in diverse contexts. Consequently, a critical area of research revolves around addressing synchronization challenges in CDNs, particularly through the incorporation of feedback control strategies. Various control approaches have emerged in the literature, including model predictive control, state feedback control, stochastic control, adaptive control, non-fragile control, and pinning control, as documented in prior research [23–27].

Real-world networks, such as mobile communication systems, citation networks, and cyber-physical setups, frequently depend on time-triggered schemes for data exchange among sensors, controllers, and actuators. However, there are disadvantages to using synchronization methods designed for complex networks with time-triggered schemes. Recent research has explored diverse aspects, including the synchronization of real-time tasks in time-triggered networks [28], adaptive pinning synchronization in networks with negative weights and its application in traffic road networks [29], enhancing security in time-triggered real-time systems through task replication [30], and achieving exponential synchronization of chaotic Lur'e systems with time-triggered intermittent control [31]. To effectively result of the burdens on communication networks, the adoption of event-triggered methodologies has emerged as a promising strategy. The fundamental premise underlying event-triggered control/communication schemes revolves around the concept that the execution of control inputs and system transmissions is dictated by the occurrence of predefined “events.” This approach is engineered to uphold the intended control performance while simultaneously alleviating the strain on communication networks [32,33].

In response to the challenges posed by communication networks, the adoption of event-triggered methodologies has emerged as a promising strategy. Event-triggered control/communication schemes

stand in contrast to conventional time-triggered approaches, effectively alleviating the strain on both network communication and controller computational costs. Existing event-triggered control techniques can typically be classified into four main categories: dynamic event-triggered control, self-triggered control, periodic event-triggered control and continuous event-triggered control. Various event-triggered synchronization control strategies tailored for complex dynamical networks have been proposed in several sources, utilizing mathematical tools such as Lyapunov stability theory, linear matrix inequalities, Markov process theory, and impulsive control theory to formulate event-triggered controllers [34–41]. For instance, in [35], a robust H_∞ pinning synchronization method for complex networks with event-triggered communication is introduced, employing Lyapunov-Krasovskii functional (LKF) and matrix inequality techniques for controller design. Similarly, [36] explores an event-triggered pinning control approach for discrete-time stochastic complex dynamical network synchronization, utilizing Markov process theory and stochastic analysis for stability analysis. Another study focuses on coupled reaction-diffusion complex network systems, applying finite-time stability theory and LKF to design event-triggered controllers, which outperform traditional continuous-time control methods [37]. Moreover, [38] suggests an event-triggered delayed impulsive control approach for CDNs with coupling delay, utilizing LKF and impulsive control theory. In [42], a dynamic event-triggered control method is introduced as an alternative to static event-triggered control systems, aiming to further reduce information usage and energy consumption. However, dynamic approaches introduce complexities such as Zeno behavior, where an infinite number of triggers occur in a finite time span, posing challenges for event-triggered control systems. Consequently, it becomes crucial for event-triggering conditions to ensure a minimum constraint on time intervals between triggering moments to prevent Zeno behavior.

Recent literature has explored the concept of dynamic event-triggered control in various contexts, as evident from works such as [43–50]. [43] likely contributes to the field by advancing dynamic event-triggered control methodologies and their applications. [45] may focus on dissipative systems, shedding light on energy-efficient control strategies. The authors in [46] explore novel triggering mechanisms and performance analyses in specific scenarios. [47] studied event-triggered control's utilization within cluster systems, optimizing resource allocation. The authors of [48] researched the balance between communication and control efficiency in event-triggered systems. The authors in [49] introduced a disturbance-based switching mechanism for robust synchronization, while [50] proposed a memory-based strategy for efficient global synchronization. These contributions expand the applicability of event-triggered control in chaotic Lurie systems, addressing challenges related to disturbances and global synchronization. It is well-known that proportional-integral-derivative (PID) controllers have been widely applied in industry for operation simplicity and good system performance. In [51], researchers utilized the linear matrix inequality technique to create an event-triggered fuzzy PID controller. This research effectively expanded the use of event-triggering mechanisms into PID control for linear time-invariant systems. However, only a few works have investigated the feasibility of PID control applied to complex networks. Motivated by the discussions above, this study aims to make significant contributions to PID control in CDNs with hybrid delays. The main contributions of this research are outlined below:

- In this paper, there is the first attempt to study a synchronization of PID control problem in CDNs by introducing a dynamic event-triggered mechanism. This novel combination aims to achieve exponential synchronization for CDNs. This contribution advances the understanding of

synchronization techniques in complex systems.

- Different from others in [52, 53], we have introduced a PID-based event-triggering mechanism inspired by the structure of the traditional PID control law. This novel mechanism takes into account the influence of the system's proportional, integral and derivative components, with parameters designed in harmony with those of the PID controller.
- To establish the theoretical support of our approach, we carefully construct a suitable LKF. We derive its properties employing linear matrix inequalities (LMI), which facilitates the analysis of the complex dynamical networks under consideration. This step is important in demonstrating the feasibility of achieving exponential synchronization within our proposed framework.
- Recognizing the significance of real-world uncertainties, we intensively look into the impact of parameter uncertainties on the considered system. Through rigorous analysis, we examine the system's exponential synchronization behavior using PID control parameters within the dynamic event-trigger mechanism. This exploration of parameter uncertainties adds a layer of practical relevance to the theoretical results.
- Finally, to show the effectiveness and validity of our theoretical contributions, we provide a comprehensive numerical simulation. This showcases practical scenarios and demonstrates the outcomes of our proposed approach.

The subsequent sections of the paper are organized as follows: Section 2 introduces essential preliminaries and presents the problem formulation. Section 3 establishes the Exponential Synchronization Criteria for general complex dynamical networks, employing the PID controller within the dynamic event-trigger mechanism. Section 4 extends the analysis by incorporating parameter uncertainties into the complex dynamical networks. This section critically examines the resulting impact on exponential synchronization. The paper concludes with Section 5, where a summary and conclusive remarks wrap up the discussion.

Notation: To be clear, the following symbols are first explained in a simple way

T : The transpose of a matrix or a vector.

\mathbb{R}^n : The n -dimensional Euclidean space.

$\mathbb{R}^{n \times m}$: The set of all $n \times m$ real matrices.

$\mathcal{W} > 0$: The matrix \mathcal{W} is symmetric and positive definite.

\star : Symmetric terms in a symmetric matrix.

I_n : Identity matrix.

$\text{diag}\{\dots\}$: A block-diagonal matrix.

$\lambda_{\max}(G)$ ($\lambda_{\min}(G)$): The largest (smallest) eigenvalue of G .

$\|\cdot\|$: The Euclidean norm for given vector.

2. Problem formulation

Consider a controlled complex network consisting of N nodes with hybrid delays [5, 16, 54]. Each node of the dynamical network is a nonautonomous n -dimensional systems, which is given by

$$\dot{x}_i(t) = \mathcal{A} x_i(t) + f(x_i(t)) + \sum_{j=1}^N \mathcal{E}_{ij} \Theta_1 x_j(t) + \sum_{j=1}^N \mathcal{H}_{ij} \Theta_2 x_j(t - \alpha(t)) + \sum_{j=1}^N \mathcal{J}_{ij} \Theta_3 \int_{t-\delta}^t x_j(s) ds$$

$$+u_i(t), \quad (2.1)$$

where $i = 1, 2, \dots, N$ is the number of nodes in the Network. $x_i(t) = \{x_{i1}(t), x_{i2}(t), \dots, x_{in}(t)\}$ is the state variable of the i^{th} node at time t . \mathcal{A} is the known state matrix. $f(\cdot) : \mathbb{R}^n \rightarrow \mathbb{R}^n$ is the nonlinear function which is continuous and differentiable that represents the dynamical behaviors of the system. The matrices \mathcal{E}_{ij} , \mathcal{H}_{ij} and \mathcal{J}_{ij} represent the outer coupling and network topology structure. When there is a direct connection from node i to node j , the values are $\mathcal{E}_{ij} > 0$, $\mathcal{H}_{ij} > 0$ and $\mathcal{J}_{ij} > 0$; otherwise, they are 0. These matrices also satisfy the conditions $\mathcal{E}_{ii} = -\sum_{j=1}^N \mathcal{E}_{ij}$, $\mathcal{H}_{ii} = -\sum_{j=1}^N \mathcal{H}_{ij}$ and $\mathcal{J}_{ii} = -\sum_{j=1}^N \mathcal{J}_{ij}$ to maintain internal consistency. Θ_1 , Θ_2 and Θ_3 represent the inner coupling matrices which interconnect the subsystems. $\alpha(t)$ is the time varying discrete delay, and δ is the distributed delay, satisfying the condition $0 \leq \alpha(t) \leq \alpha$ and $0 \leq \dot{\alpha}(t) \leq \zeta \leq 1$. $u_i(t)$ is the control input to be designed.

Now, consider the reference node $S(t) \in \mathbb{R}^n$ in the form which satisfies

$$\dot{S}(t) = \mathcal{A}S(t) + f(S(t)). \quad (2.2)$$

Define the synchronization error as $\dot{\varphi}_i(t) = \dot{x}_i(t) - \dot{S}(t)$. Then, by subtracting (2.2) from (2.1), we have the dynamical error system as:

$$\begin{aligned} \dot{\varphi}_i(t) &= \mathcal{A}\varphi_i(t) + \mathcal{G}(\varphi_i(t)) + \sum_{j=1}^N \mathcal{E}_{ij}\Theta_1\varphi_j(t) + \sum_{j=1}^N \mathcal{H}_{ij}\Theta_2\varphi_j(t - \alpha(t)) \\ &\quad + \sum_{j=1}^N \mathcal{J}_{ij}\Theta_3 \int_{t-\delta}^t \varphi_j(s)ds + u_i(t), \end{aligned} \quad (2.3)$$

where $\mathcal{G}(\varphi_i(t)) = [f(x_i(t)) - f(S(t))]$. For general complex dynamical networks with network topologies, we propose PID control protocols, which are described by

$$\Psi_i(t) = \mathcal{U}_P\varphi_i(t) + \mathcal{U}_I \int_0^t \varphi_i(s)ds + \mathcal{U}_D\dot{\varphi}_i(t), \quad (2.4)$$

where $\mathcal{U}_P > 0$, $\mathcal{U}_I > 0$ and $\mathcal{U}_D > 0$ are the proportional, integral and derivative control gain values, respectively, which are to be designed for the i^{th} node.

Remark 2.1. *PID control is a well known effective approach to various real-world control challenges. It is referred to as a universal controller because the proportional gain \mathcal{U}_P increases control effort when there is a significant control error-making its function quite clear. With the integral action (\mathcal{U}_I), the subsequent control uses previous control error values, and the derivative gain (\mathcal{U}_D) relies on expectations of future error values. In a dynamic event-triggered control system, the main goal is to minimize information and energy sources. The PID controller plays a crucial role by boosting control efforts when errors are significant, fitting well with the dynamic nature of the CDNs. Adding the integral action lets the control system learn from past data, and the derivative gain helps predict future errors—useful for navigating the changing dynamics of complex networks. In dynamic event-triggered control systems, PID works smoothly, making decisions that align with the goal of minimizing information use.*

In order to reduce the communication burden of the shared network in the control process, in this paper, a dynamic event-triggered mechanism is introduced to judge when the measured data should be

transmitted to the observer. For clarity of the dynamic event-triggered mechanism, let us define the triggering time sequence for the i^{th} node iteratively expressed as $t_{k+1}^i = \inf\{t > t_k^i | \mathcal{L}_i(t) < 0\}$, and the event generator function $\mathcal{L}_i(\cdot)$ can be taken from [55] and can be given by

$$\mathcal{L}_i(t) = \frac{1}{v_i} \mathcal{D}_i(t) + \mu_i \Psi_i^T(t) \Psi_i(t) - \omega_i^T(t) \omega_i(t), \quad (2.5)$$

where v_i and μ_i are two given positive scalars. For $t \in [t_k^i, t_{k+1}^i)$, $\omega_i(t)$ is defined by,

$$\omega_i(t) = \Psi_i(t) - \Psi_i(t_k^i), \quad (2.6)$$

where $\Psi_i(t_k^i)$ is the i^{th} node of the control signal at the earliest triggering instant. The triggering instants are denoted by $\{t_k^i\}_{k=0}^{\infty}$ and $t_0^i = 0$. Also, the internal dynamic variable $\mathcal{D}_i(t)$ should satisfy

$$\dot{\mathcal{D}}_i(t) = -\rho_i \mathcal{D}_i(t) - \omega_i^T(t) \omega_i(t) + \mu_i \Psi_i^T(t) \Psi_i(t). \quad (2.7)$$

Here, ρ_i is the scalar value. From the above equation, $\mathcal{D}_i(0) > 0$ is the initial condition. Moreover, for all $t \geq 0$,

$$\dot{\mathcal{D}}_i(t) \geq -\rho_i \mathcal{D}_i(t) - \frac{1}{v_i} \mathcal{D}_i(t).$$

By using this, we can easily obtain

$$\mathcal{D}_i(t) \geq \mathcal{D}_i(0) e^{-(\rho_i + \frac{1}{v_i})t} > 0.$$

For the i^{th} node, the actual input actuator can be chosen as

$$u_i(t) = u_i(t_k^i) = -\Psi_i(t_k^i), \quad \forall t \in [t_k^i, t_{k+1}^i). \quad (2.8)$$

The following error dynamic system can be obtained by applying (2.6) and (2.8) to the error system (2.3):

$$\begin{aligned} \dot{\varphi}_i(t) = & \mathcal{A} \varphi_i(t) + \mathcal{G}(\varphi_i(t)) + \sum_{j=1}^N \mathcal{E}_{ij} \Theta_1 \varphi_j(t) + \sum_{j=1}^N \mathcal{H}_{ij} \Theta_2 \varphi_j(t - \alpha(t)) \\ & + \sum_{j=1}^N \mathcal{I}_{ij} \Theta_3 \int_{t-\delta}^t \varphi_j(s) ds - \Psi_i(t) + \omega_i(t). \end{aligned} \quad (2.9)$$

By (2.4) and the system (2.9), we can obtain the following:

$$\begin{aligned} \dot{\varphi}_i(t) = & \mathcal{A} \varphi_i(t) + \mathcal{G}(\varphi_i(t)) + \sum_{j=1}^N \mathcal{E}_{ij} \Theta_1 \varphi_j(t) + \sum_{j=1}^N \mathcal{H}_{ij} \Theta_2 \varphi_j(t - \alpha(t)) \\ & + \sum_{j=1}^N \mathcal{I}_{ij} \Theta_3 \int_{t-\delta}^t \varphi_j(s) ds - \mathcal{U}_{iP} \varphi_i(t) - \mathcal{U}_{iI} \int_0^t \varphi_i(s) ds - \mathcal{U}_{iD} \dot{\varphi}_i(t) + \omega_i(t). \end{aligned} \quad (2.10)$$

The error system can be written in compact form as

$$\begin{aligned} \dot{\varphi}(t) = & \mathcal{A}\varphi(t) + \mathcal{G}(\varphi(t)) + (\mathcal{E} \otimes \Theta_1)\varphi(t) - (\mathcal{H} \otimes \Theta_2)\varphi(t - \alpha(t)) + (\mathcal{J} \otimes \Theta_3) \int_{t-\delta}^t \varphi(s)ds - \mathcal{U}_P\varphi(t) \\ & - \mathcal{U}_I \int_0^t \varphi(s)ds - \mathcal{U}_D\dot{\varphi}(t) + \omega(t). \end{aligned} \quad (2.11)$$

The upcoming Assumptions, Lemmas and Definitions are very useful to prove our theoretical results.

Assumption H1. [55] The nonlinear function $f(\cdot) : \mathbb{R}^n \rightarrow \mathbb{R}^n$ satisfies the following the sector-bounded condition:

$$[f(x) - f(y) - \Upsilon_1(x - y)]^T [f(x) - f(y) - \Upsilon_2(x - y)] \leq 0,$$

for any $x, y \in \mathbb{R}^n$, where Υ_1 and Υ_2 are known constant matrices.

Lemma 2.2. [55] The following inequality holds for the **H1**, for the matrices Υ_1 and Υ_2 such that

$$\begin{bmatrix} \varphi(t) \\ \mathcal{G}(\varphi(t)) \end{bmatrix}^T \begin{bmatrix} \widehat{\Upsilon}_1 & \widehat{\Upsilon}_2 \\ * & I \end{bmatrix} \begin{bmatrix} \varphi(t) \\ \mathcal{G}(\varphi(t)) \end{bmatrix} \leq 0,$$

where

$$\widehat{\Upsilon}_1 = \frac{(I_N \otimes \Upsilon_1)^T (I_N \otimes \Upsilon_2) + (I_N \otimes \Upsilon_2)(I_N \otimes \Upsilon_1)^T}{2}, \quad \widehat{\Upsilon}_2 = \frac{(I_N \otimes \Upsilon_2)^T + (I_N \otimes \Upsilon_1)^T}{2}.$$

Lemma 2.3. (Schur Complement) [56] The LMI, $\mathcal{U} = \begin{bmatrix} \mathcal{U}_{11} & \mathcal{U}_{12} \\ \mathcal{U}_{21} & \mathcal{U}_{22} \end{bmatrix} < 0$, is equivalent to $\mathcal{U}_{22} < 0$,

$$\mathcal{U}_{11} - \mathcal{U}_{12}\mathcal{U}_{22}^{-1}\mathcal{U}_{12}^T < 0.$$

Definition 2.4. [57] The complex dynamical network with hybrid delays (2.1) is said to be exponentially synchronized with target node (2.2) if there exists two constants $\epsilon > 0$ and $M > 0$ such that

$$\|x_i(t) - S(t)\| \leq Me^{-\epsilon t}, \quad i = 1, 2, \dots, N,$$

for $t \geq 0$ and any initial conditions.

The goal of this research is to develop a set of PID controllers (2.4) in order to guarantee the exponential synchronization of the CDNs (2.1) and response system (2.2). Specifically, we are interest in if the CDN with hybrid delay error system (2.11) is exponentially stable.

3. Main results

The following theorems, when applied to a dynamic event-triggered PID control method with linear matrix inequalities, would enforce the appropriate exponential synchronization of CDNs with hybrid delays.

Theorem 3.1. If given parameters $\alpha, \varsigma \leq 1, \rho, \mu, \nu, \beta, \mathcal{U}_P, \mathcal{U}_I$ and \mathcal{U}_D and the Assumption **H1** are true, then the CDN (2.1) is said to be exponentially synchronized with (2.2) if there exist positive definite matrices \mathcal{C}_r ($r = 1, 2, \dots, 5$), $\mathcal{B}_1, \mathcal{B}_2$ and $\mathcal{W}_a = \begin{bmatrix} \mathcal{W}_1 & \mathcal{W}_2 \\ \mathbf{\boxtimes} & \mathcal{W}_3 \end{bmatrix} > 0, \mathcal{W}_b = \begin{bmatrix} \mathcal{W}_4 & \mathcal{W}_5 \\ \mathbf{\boxtimes} & \mathcal{W}_6 \end{bmatrix} > 0$ and appropriate dimension matrices \mathcal{N}_r ($r = 1, 2, \dots, 8$) and positive scalars ε_1 and ε_2 , such that the following LMIs hold:

$$\mathfrak{J} = \begin{bmatrix} \mathfrak{J}_{11 \times 11} \end{bmatrix} < 0, \quad (3.1)$$

where matrix entries are provided as follows, with any missing entries assumed to be zero:

$$\begin{aligned} \mathfrak{J}_{11} &= (\mathcal{B}_1 + \mathcal{B}_1^T) + \mathcal{C}_1 + \mathcal{C}_2 + \mathcal{B}_2 + \varsigma \mathcal{C}_5 + 2\beta \mathcal{B}_1 + 2\beta \mathcal{W}_1 + 2\beta \mathcal{W}_4 + \mathcal{U}_P^T \Xi_1 \mathcal{U}_P + 2 \left[\mathcal{N}_1 \mathcal{A} + \mathcal{N}_1 (\mathcal{E} \otimes \Theta_1) - \mathcal{N}_1 \mathcal{U}_P \right] + \varepsilon_1 \mathcal{U}_P^T \Xi_3 \mathcal{U}_P - \varepsilon_2 \widehat{\Upsilon}_1; \mathfrak{J}_{12} = 2\beta \mathcal{W}_2^T + \mathcal{N}_1^T (\mathcal{H} \otimes \Theta_2)^T + \mathcal{N}_2 \left[\mathcal{A} + (\mathcal{E} \otimes \Theta_1) - 2\mathcal{U}_P \right]; \\ \mathfrak{J}_{13} &= \mathcal{U}_P^T \Xi_1 \mathcal{U}_I - \mathcal{N}_1 \mathcal{U}_I + \mathcal{N}_3 \left[\mathcal{A} + (\mathcal{E} \otimes \Theta_1) - \mathcal{U}_P \right] + 2\varepsilon_1 \mathcal{U}_P^T \Xi_3 \mathcal{U}_I; \mathfrak{J}_{14} = \mathcal{B}_1 + \mathcal{W}_1^T + \mathcal{W}_4^T + \mathcal{U}_P^T \Xi_1 \mathcal{U}_D - \left[\mathcal{N}_1 \mathcal{U}_D + \mathcal{N}_1 \right] + \mathcal{N}_4 \left[\mathcal{A} + (\mathcal{E} \otimes \Theta_1) - \mathcal{U}_P \right] + 2\varepsilon_1 \mathcal{U}_P^T \Xi_3 \mathcal{U}_D; \mathfrak{J}_{15} = (1 - \varsigma) \mathcal{W}_3 + \mathcal{N}_5 \left[\mathcal{A} + (\mathcal{E} \otimes \Theta_1) - \mathcal{U}_P \right]; \\ \mathfrak{J}_{16} &= \mathcal{N}_1 (\mathcal{J} \otimes \Theta_3) + \mathcal{N}_6 \left[\mathcal{A} + (\mathcal{E} \otimes \Theta_1) - \mathcal{U}_P \right]; \mathfrak{J}_{17} = \mathcal{N}_7 \left[\mathcal{A} + (\mathcal{E} \otimes \Theta_1) - \mathcal{U}_P \right] + 2\beta \mathcal{W}_5; \mathfrak{J}_{18} = \mathcal{W}_5^T + \mathcal{N}_8 \left[\mathcal{A} + (\mathcal{E} \otimes \Theta_1) - \mathcal{U}_P \right]; \mathfrak{J}_{19} = \mathcal{N}_1^T; Y_{110} = \mathcal{N}_1^T - \varepsilon_2 \widehat{\Upsilon}_2; \mathfrak{J}_{22} = -e^{-2\beta\varsigma} (1 - \varsigma) \mathcal{C}_2 + 2\beta \mathcal{W}_3 + \mathcal{N}_2 (\mathcal{H} \otimes \Theta_2); \\ \mathfrak{J}_{23} &= \mathcal{N}_2 \mathcal{U}_I + \mathcal{N}_3 (\mathcal{H} \otimes \Theta_2); \mathfrak{J}_{24} = \mathcal{W}_2 - \left[\mathcal{N}_2 + \mathcal{N}_2 \mathcal{U}_D \right] + \mathcal{N}_4 (\mathcal{H} \otimes \Theta_2); \mathfrak{J}_{25} = (1 - \varsigma) \mathcal{W}_3 + \mathcal{N}_5 (\mathcal{H} \otimes \Theta_2); \\ \mathfrak{J}_{26} &= \mathcal{N}_2 (\mathcal{J} \otimes \Theta_3) + \mathcal{N}_6 \left[\mathcal{H} \otimes \Theta_2 \right]; \mathfrak{J}_{27} = \mathcal{N}_7 (\mathcal{H} \otimes \Theta_2); \mathfrak{J}_{28} = \mathcal{N}_8 (\mathcal{H} \otimes \Theta_2); \mathfrak{J}_{29} = \mathcal{N}_2^T; \mathfrak{J}_{210} = \mathcal{N}_2^T; \\ \mathfrak{J}_{33} &= \mathcal{U}_I^T \Xi_1 \mathcal{U}_I - 2\mathcal{N}_3 \mathcal{U}_I + \varepsilon_1 \mathcal{U}_I^T \Xi_3 \mathcal{U}_I; \mathfrak{J}_{34} = \mathcal{U}_I^T \Xi_1 \mathcal{U}_D - \left[\mathcal{N}_3 \mathcal{U}_D + \mathcal{N}_3 \right] + \varepsilon_1 + \mathcal{U}_I^T \Xi_3 \mathcal{U}_D - \mathcal{N}_4 \mathcal{U}_I; \\ \mathfrak{J}_{35} &= -\mathcal{N}_5 \mathcal{U}_I; \mathfrak{J}_{36} = \mathcal{N}_3 \left[\mathcal{J} \otimes \Theta_3 \right] - \mathcal{N}_6 \mathcal{U}_I; \mathfrak{J}_{37} = -\mathcal{N}_7 \mathcal{U}_I; \mathfrak{J}_{38} = -\mathcal{N}_8 \mathcal{U}_I; \mathfrak{J}_{39} = \mathcal{N}_3^T; \mathfrak{J}_{310} = \mathcal{N}_3^T; \\ \mathfrak{J}_{44} &= \mathcal{U}_D^T \Xi_1 \mathcal{U}_D + \mathcal{C}_3 + \mathcal{C}_4 - 2 \left[\mathcal{N}_4 \mathcal{U}_D + \mathcal{N}_4 \right] + \varepsilon_1 \mathcal{U}_D^T \Xi_2 \mathcal{U}_D; \mathfrak{J}_{45} = - \left[\mathcal{N}_5 \mathcal{U}_D + \mathcal{N}_5 \right]; \mathfrak{J}_{46} = \mathcal{N}_4 (\mathcal{J} \otimes \Theta_3) - \left[\mathcal{N}_6 \mathcal{U}_D + \mathcal{N}_6 \right]; \\ \mathfrak{J}_{47} &= \mathcal{W}_5^T - \left[\mathcal{N}_7 \mathcal{U}_D + \mathcal{N}_7 \right]; \mathfrak{J}_{48} = \left[\mathcal{N}_8 \mathcal{U}_D + \mathcal{N}_8 \right]; \mathfrak{J}_{49} = \mathcal{N}_4^T; \mathfrak{J}_{410} = \mathcal{N}_4^T; \\ \mathfrak{J}_{55} &= -(1 - \varsigma) e^{-2\beta\varsigma} \mathcal{C}_4; \mathfrak{J}_{56} = \mathcal{N}_5 (\mathcal{J} \otimes \Theta_3); \mathfrak{J}_{59} = \mathcal{N}_5^T; \mathfrak{J}_{510} = \mathcal{N}_5^T; \mathfrak{J}_{66} = -\frac{e^{-2\beta\varsigma}}{\delta} \mathcal{C}_5 + \mathcal{N}_6 (\mathcal{J} \otimes \Theta_3); \\ \mathfrak{J}_{67} &= \mathcal{N}_7 (\mathcal{J} \otimes \Theta_3); \mathfrak{J}_{68} = \mathcal{N}_8 (\mathcal{J} \otimes \Theta_3); Y_{69} = \mathcal{N}_6^T; Y_{610} = \mathcal{N}_6^T; \mathfrak{J}_{77} = -e^{-2\beta\varsigma} \mathcal{C}_1 + 2\beta \mathcal{W}_6; \mathfrak{J}_{78} = \mathcal{W}_5^T; \\ \mathfrak{J}_{79} &= \mathcal{N}_7^T; \mathfrak{J}_{710} = \mathcal{N}_7^T; \mathfrak{J}_{88} = -e^{-2\beta\varsigma} \mathcal{C}_3; \mathfrak{J}_{89} = \mathcal{N}_8^T; \mathfrak{J}_{810} = \mathcal{N}_8^T; \mathfrak{J}_{99} = -\Xi_1 - \varepsilon_1 I; \mathfrak{J}_{1010} = -\varepsilon_2 I; \\ \mathfrak{J}_{1111} &= \text{diag} \left\{ \frac{-\rho_1 + 2\beta + \mu_1}{v_1}, \frac{-\rho_2 + 2\beta + \mu_1}{v_2}, \frac{-\rho_N + 2\beta + \mu_1}{v_N} \right\}, \\ \Xi_1 &= \text{diag} \left\{ \frac{1}{v_1} I, \frac{1}{v_2} I, \dots, \frac{1}{v_N} I \right\}, \Xi_2 = \text{diag} \left\{ \frac{\mu_1}{v_1} I, \frac{\mu_2}{v_2} I, \dots, \frac{\mu_N}{v_N} I \right\}, \Xi_3 = \text{diag} \left\{ \mu_1 I, \mu_2 I, \dots, \mu_N I \right\}. \end{aligned}$$

Proof. Consider the Lyapunov function according to the error system (2.11) that can be given by

$$V(t) = \sum_{i=1}^7 V_i(t), \quad (3.2)$$

where

$$\begin{aligned}
 V_1(t) &= \varphi^T(t) \mathcal{B}_1 \varphi(t), \\
 V_2(t) &= \begin{bmatrix} \varphi^T(t) & \varphi^T(t - \alpha(t)) \end{bmatrix} \begin{bmatrix} \mathcal{W}_1 & \mathcal{W}_2 \\ \mathcal{X} & \mathcal{W}_3 \end{bmatrix} \begin{bmatrix} \varphi(t) \\ \varphi(t - \alpha(t)) \end{bmatrix}, \\
 V_3(t) &= \begin{bmatrix} \varphi^T(t) & \varphi^T(t - \alpha) \end{bmatrix} \begin{bmatrix} \mathcal{W}_4 & \mathcal{W}_5 \\ \mathcal{X} & \mathcal{W}_6 \end{bmatrix} \begin{bmatrix} \varphi(t) \\ \varphi(t - \alpha) \end{bmatrix}, \\
 V_4(t) &= \int_{t-\varsigma}^t e^{2\beta(s-t)} \varphi^T(v) \mathcal{C}_1 \varphi(v) dv + \int_{t-\alpha(t)}^t e^{2\beta(s-t)} \varphi^T(v) \mathcal{C}_2 \varphi(v) dv, \\
 V_5(t) &= \int_{t-\varsigma}^t e^{2\beta(s-t)} \dot{\varphi}^T(v) \mathcal{C}_3 \dot{\varphi}(v) dv + \int_{t-\alpha(t)}^t e^{2\beta(s-t)} \dot{\varphi}^T(v) \mathcal{C}_4 \dot{\varphi}(v) dv, \\
 V_6(t) &= \int_0^t e^{2\beta(s-t)} \varphi^T(v) \mathcal{B}_2 \varphi(v) dv + \int_{-\delta}^0 \int_{t+\theta}^t e^{2\beta(s-t)} \varphi^T(v) \mathcal{C}_5 \varphi(v) dv d\theta, \\
 V_7(t) &= \sum_{i=1}^N \frac{1}{v_i} \mathcal{D}_i(t).
 \end{aligned}$$

Hereafter, let us consider the following notations:

$$\begin{aligned}
 Y_1(t) &= \varphi(t); \quad Y_2(t) = \varphi(t - \alpha(t)); \quad Y_3(t) = \int_0^t \varphi(v) dv; \quad Y_4(t) = \dot{\varphi}(t); \quad Y_5(t) = \dot{\varphi}(t - \alpha(t)); \\
 Y_6(t) &= \int_{t-\delta}^t \varphi(v) dv; \quad Y_7(t) = \varphi(t - \alpha); \quad Y_8(t) = \dot{\varphi}(t - \alpha).
 \end{aligned}$$

Now, taking the derivative of the considered Lyapunov function can be given by

$$\dot{V}_1(t) + 2\beta V_1(t) = 2Y_1^T(t) \mathcal{B}_1 Y_4(t) + 2\beta Y_1^T(t) \mathcal{B}_1 Y_1(t), \quad (3.3)$$

$$\begin{aligned}
 \dot{V}_2(t) + 2\beta V_2(t) &= 2Y_1^T(t) \mathcal{W}_1 Y_4(t) + 2Y_2^T(t) \mathcal{W}_2^T Y_4(t) + 2(1 - \varsigma) Y_1^T \mathcal{W}_2 Y_5(t) \\
 &\quad + 2(1 - \varsigma) Y_2^T(t) \mathcal{W}_3 Y_5(t) + 2\beta Y_1^T(t) \mathcal{W}_1 Y_1(t) + 4\beta Y_1^T(t) \mathcal{W}_2 Y_2(t) \\
 &\quad + 2\beta Y_2^T(t) \mathcal{W}_3 Y_2(t),
 \end{aligned} \quad (3.4)$$

$$\begin{aligned}
 \dot{V}_3(t) + 2\beta V_3(t) &= 2Y_1^T(t) \mathcal{W}_4 Y_4(t) + 2Y_7^T(t) \mathcal{W}_5^T Y_4(t) + 2Y_1^T \mathcal{W}_5 Y_8(t) + 2Y_7^T(t) \mathcal{W}_6 Y_8(t) \\
 &\quad + 2\beta Y_1^T(t) \mathcal{W}_4 Y_1(t) + 4\beta Y_1^T(t) \mathcal{W}_5 Y_7(t) + 2\beta Y_7^T(t) \mathcal{W}_6 Y_7(t),
 \end{aligned} \quad (3.5)$$

$$\begin{aligned}
 \dot{V}_4(t) + 2\beta V_4(t) &= Y_1^T(t) \mathcal{C}_1 Y_1(t) - e^{-2\beta\varsigma} Y_7^T(t) \mathcal{C}_1 Y_7(t) \\
 &\quad + Y_1^T(t) \mathcal{C}_2 Y_1(t) - e^{-2\beta\varsigma} (1 - \varsigma) Y_2^T \mathcal{C}_2 Y_2(t),
 \end{aligned} \quad (3.6)$$

$$\begin{aligned}
 \dot{V}_5(t) + 2\beta V_5(t) &= Y_4^T(t) \mathcal{C}_3 Y_4(t) - e^{-2\beta\varsigma} Y_8^T(t) \mathcal{C}_3 Y_8(t) \\
 &\quad + Y_4^T(t) \mathcal{C}_4 Y_4(t) - e^{-2\beta\varsigma} (1 - \varsigma) Y_5^T(t) \mathcal{C}_4 Y_5(t),
 \end{aligned} \quad (3.7)$$

$$\dot{V}_6(t) + 2\beta V_6(t) = Y_1^T(t) \mathcal{B}_2 Y_1(t) + \varsigma Y_1^T(t) \mathcal{C}_5 Y_1(t) - e^{-2\beta\varsigma} \int_{t-\delta}^t \varphi^T(v) \mathcal{C}_5 \varphi(v) dv, \quad (3.8)$$

$$\begin{aligned}
 \dot{V}_7(t) + 2\beta V_7(t) &= \sum_{i=1}^N \frac{1}{v_i} \dot{\mathcal{D}}_i(t) + 2\beta V_7(t), \\
 &= \sum_{i=1}^N \frac{1}{v_i} \left[-\rho_i \mathcal{D}_i(t) - \omega^T(t) \omega(t) + \mu_i \Psi_i^T(t) \Psi_i(t) \right] + 2\beta \sum_{i=1}^N \frac{1}{v_i} \mathcal{D}_i(t),
 \end{aligned}$$

$$\begin{aligned}
&= \sum_{i=1}^N \frac{-\rho_i}{v_i} \mathcal{D}_i(t) - \omega^T(t) i_2 \omega(t) + \varphi^T(t) \mathcal{U}_P^T \Xi_1 \mathcal{U}_P \varphi(t) + \int_0^t \varphi^T(v) dv \mathcal{U}_I^T \Xi_1 \mathcal{U}_I \int_0^t \varphi(v) dv \\
&\quad + \dot{\varphi}^T(t) \mathcal{U}_D^T \Xi_1 \mathcal{U}_D \dot{\varphi}(t) + 2\varphi^T(t) \mathcal{U}_P^T \Xi_1 \mathcal{U}_I \int_0^t \varphi(v) dv + 2\varphi^T(t) \mathcal{U}_P^T \Xi_1 \mathcal{U}_D \dot{\varphi}(t) \\
&\quad + 2 \int_0^t \varphi^T(v) dv \mathcal{U}_I^T \Xi_1 \mathcal{U}_D \dot{\varphi}(t) + 2\beta \sum_{i=1}^N \frac{1}{v_i} \mathcal{D}_i(t), \\
&= - \sum_{i=1}^N \frac{\rho_i}{v_i} \mathcal{D}_i(t) - \omega^T(t) \Xi_2 \omega(t) + Y_1^T(t) \mathcal{U}_P^T \Xi_1 \mathcal{U}_P Y_1(t) + Y_3^T(t) \mathcal{U}_I^T \Xi_1 \mathcal{U}_I Y_3(t) \\
&\quad + Y_4^T(t) \mathcal{U}_D^T \Xi_1 \mathcal{U}_D Y_4(t) + 2Y_1^T(t) \mathcal{U}_P^T \Xi_1 \mathcal{U}_I Y_3(t) + 2Y_1^T(t) \mathcal{U}_P^T \Xi_1 \mathcal{U}_D Y_4(t) \\
&\quad + 2Y_3^T(t) \mathcal{U}_I^T \Xi_1 \mathcal{U}_D Y_4(t) + 2\beta \sum_{i=1}^N \frac{1}{v_i} \mathcal{D}_i(t), \tag{3.9}
\end{aligned}$$

where $\Xi_1 = \text{diag}\{\frac{\mu_1}{v_1}, \frac{\mu_2}{v_2}, \dots, \frac{\mu_M}{v_M}\}$ and $\Xi_2 = \text{diag}\{\frac{1}{v_1}, \frac{1}{v_2}, \dots, \frac{1}{v_M}\}$.

From (3.8), using Jensen's inequality, we can get the following inequality:

$$- \int_{t-\delta}^t \varphi^T(v) \mathcal{L}_5 \varphi(v) dv \leq -\frac{1}{\delta} \left(\int_{t-\delta}^t \varphi(v) dv \right) \mathcal{L}_5 \left(\int_{t-\delta}^t \varphi(v) dv \right). \tag{3.10}$$

From (2.5) and $\mathcal{L}_i(t) < 0$, we can get

$$\sum_{i=1}^N \frac{1}{v_i} \mathcal{D}_i(t) + \sum_{i=1}^N \mu_i \Psi_i^T(t) \Psi_i(t) - \sum_{i=1}^N \omega_i^T(t) \omega_i(t) \geq 0. \tag{3.11}$$

Any scalar ε_1 that there exists can be obtained using the inequality above.

$$\begin{aligned}
0 \leq \varepsilon_1 \sum_{i=1}^N \frac{1}{v_i} \mathcal{D}_i(t) - \varepsilon_1 \omega^T(t) \omega(t) + \varepsilon_1 Y_1^T(t) \mathcal{U}_P^T \Xi_3 \mathcal{U}_P Y_1(t) + \varepsilon_1 Y_3^T(t) \mathcal{U}_I^T \Xi_3 \mathcal{U}_I Y_3(t) \\
+ \varepsilon_1 Y_4^T(t) \mathcal{U}_D^T \Xi_3 \mathcal{U}_D Y_4(t) + 2\varepsilon_1 Y_1^T(t) \mathcal{U}_P^T \Xi_3 \mathcal{U}_I Y_3(t) + 2\varepsilon_1 Y_1^T(t) \mathcal{U}_P^T \Xi_3 \mathcal{U}_D Y_4(t) \\
+ 2\varepsilon_1 Y_3^T(t) \mathcal{U}_I^T \Xi_3 \mathcal{U}_D Y_4(t), \tag{3.12}
\end{aligned}$$

where $\Xi_3 = \text{diag}\{\mu_1 I, \mu_2 I, \dots, \mu_N I\}$.

We can obtain the following from Lemma 2.2 and any scalar ε_2 :

$$-2\varepsilon_2 Y_1^T(t) \widehat{\Upsilon}_2(\mathcal{G}(\varphi(t))) - \varepsilon_2 Y_1^T(t) \widehat{\Upsilon}_1 Y_1(t) - \varepsilon_2 (\mathcal{G}^T(\varphi(t))) (\mathcal{G}(\varphi(t))) \leq 0. \tag{3.13}$$

It is evident that $0 = \dot{\varphi}(t) - Y_4(t)$, and the following equality exists for any free-weighting matrices \mathcal{N}_r , ($r = 1, 2, \dots, 8$):

$$\begin{aligned}
0 = 2 \left[Y_1^T(t) \mathcal{N}_1 + Y_2^T(t) \mathcal{N}_2 + Y_3^T(t) \mathcal{N}_3 + Y_4^T(t) \mathcal{N}_4 + Y_5^T(t) \mathcal{N}_5 + Y_6^T(t) \mathcal{N}_6 + Y_7^T(t) \mathcal{N}_7 \right. \\
\left. + Y_8^T(t) \mathcal{N}_8 \right] \times \left[\mathcal{A} \varphi(t) + (\mathcal{G}(\varphi(t))) + (\mathcal{E} \otimes \Theta_1) \varphi(t) + (\mathcal{H} \otimes \Theta_2) \varphi(t - \alpha(t)) \right]
\end{aligned}$$

$$+ (\mathcal{J} \otimes \Theta_3) \int_{t-\delta}^t \varphi(v) dv - \Psi(t) + \omega(t) - Y_4(t) \Big]. \quad (3.14)$$

Now, combining the equations from (3.2)–(3.14), we have the following inequality:

$$\dot{V}(t) + 2\beta V(t) \leq \Sigma^T(t) \mathfrak{S} \Sigma(t), \quad (3.15)$$

where

$$\Sigma(t) = \begin{bmatrix} Y_1^T(t) & Y_2^T(t) & Y_3^T(t) & Y_4^T(t) & Y_5^T(t) & Y_6^T(t) & Y_7^T(t) & Y_8^T(t) & \omega^T(t) & (\mathcal{G}^T(\varphi(t))) & \bar{\mathcal{D}}^T(t) \end{bmatrix}$$

$$\text{and } \bar{\mathcal{D}}(t) = \begin{bmatrix} \mathcal{D}_1^{\frac{1}{2}}(t) & \mathcal{D}_2^{\frac{1}{2}}(t) & \dots & \mathcal{D}_N^{\frac{1}{2}}(t) \end{bmatrix}^T.$$

Now, we can easily obtain that

$$\dot{V}(t) + 2\beta V(t) \leq 0.$$

Following a similar line as in [58], we have

$$V(0) \leq \Lambda \|\varphi(0)\|^2, \quad (3.16)$$

where

$$\begin{aligned} \Lambda = & \lambda_{\max}(\mathcal{B}_1) + \lambda_{\max}(\mathcal{W}_a) + \lambda_{\max}(\mathcal{W}_b) + \varsigma \lambda_{\max}(\mathcal{C}_1) + \varsigma \lambda_{\max}(\mathcal{C}_2) + \varsigma \lambda_{\max}(\mathcal{C}_3) \\ & + \varsigma \lambda_{\max}(\mathcal{C}_4) + \lambda_{\max}(\mathcal{B}_2) + \delta^2 \lambda_{\max}(\mathcal{C}_5). \end{aligned}$$

It becomes known that

$$V(t) \leq V(0)e^{-2\beta t} \leq \left(\Lambda \|\varphi(0)\|^2 + \sum_{i=1}^N \frac{1}{v_i} \mathcal{D}_i(0) \right) e^{-2\beta t}. \quad (3.17)$$

On the other hand,

$$V(t) \geq e^{2\beta t} \varphi^T(t) \mathcal{B}_1 \varphi(t) \geq e^{2\beta t} \lambda_{\min} \mathcal{B}_1 \|\varphi(t)\|^2. \quad (3.18)$$

Thus, one has

$$\|\varphi(t)\| \leq \sqrt{\frac{\Lambda \|\varphi(0)\|^2 + \sum_{i=1}^N \frac{1}{v_i} \mathcal{D}_i(0)}{\lambda_{\min}(\mathcal{B}_1)}} e^{-\beta t}. \quad (3.19)$$

As a result, it completes the proof of Theorem 3.1. Therefore, from Definition 2.4 we see that the CDNs (2.1) and (2.2) are exponentially synchronized and demonstrate that the CDN error (2.11) is exponentially stable.

Remark 3.2. Excluding Zeno Behavior: We need to analyze whether the system has a minimum event-triggered time interval strictly greater than zero, which means that there is no Zeno behavior. Assume that there exists Zeno behavior for at the i^{th} node, which implies that there exists $0 < T < \infty$ such that $\lim_{k \rightarrow \infty} t_k^i = T$, where T is a positive constant.

From (3.17) we know that there exists a positive constant $M_0 > 0$ such that $|\varphi_i(t)| \leq M_0$ for all $t \geq 0$ and $i = 1, 2, \dots, n$. Then, we have $|u_i(t)| \leq 2M_0\Psi_i$.

Let $\xi_0 = \frac{\sqrt{\mathcal{D}_i(0)}}{4\Psi_i M_0 \sqrt{v_i}} e^{-\frac{1}{2}(\rho_i + \frac{1}{v_i})T} > 0$. Then, from the property of limits, there exists a positive integer $N(\xi_0)$ such that $t_k^i \in [T - \xi_0, T]$, $\forall k \geq N(\xi_0)$.

By the triggering instant t_k^i and event-triggered condition with $\mathcal{L}_i(t) > 0$, we can get the following:
 $|\varphi_i(t)| \leq \frac{\sqrt{\mathcal{D}_i(0)}}{\sqrt{v_i\Psi_i}} e^{-\frac{1}{2}(\rho_i + \frac{1}{v_i})t} > 0$.

Given $|u_i(t)| \leq 2M_0\Psi_i$ and $|\varphi_i(t_k^i)| = 0$ for any triggering time t_k^i , we conclude that the sufficient condition to the above inequality is

$$(t - t_k^i)2M_0\Psi_i \leq \frac{\sqrt{\mathcal{D}_i(0)}}{\sqrt{v_i\Psi_i}} e^{-\frac{1}{2}(\rho_i + \frac{1}{v_i})t}.$$

This leads to

$$\begin{aligned} t_{N(\xi_0)+1}^i - t_{N(\xi_0)}^i &\geq \frac{\sqrt{\mathcal{D}_i(0)}}{2\Psi_i M_0 \sqrt{v_i}} e^{-\frac{1}{2}(\rho_i + \frac{1}{v_i})t_{N(\xi_0)+1}^i}, \\ &\geq \frac{\sqrt{\mathcal{D}_i(0)}}{2\Psi_i M_0 \sqrt{v_i}} e^{-\frac{1}{2}(\rho_i + \frac{1}{v_i})T} = 2\xi_0. \end{aligned}$$

This contradicts the condition $t_k^i \in [T - \xi_0, T]$, $\forall k \geq N(\xi_0)$. Therefore, Zero behavior is excluded.

In the next subsection we will investigate the uncertain CDNs with hybrid delays, and finding the results of the CDNs with given PID control parameters leading to exponential synchronization. Linear matrix inequalities are employed to accommodate uncertainties.

3.1. Complex dynamical networks with coupling parameter uncertainties using PID controller

Consider the error CDNs (2.10) involving coupling uncertainties. In this context, replace the matrices $\mathcal{A}, \Theta_1, \Theta_2$ and Θ_3 with $A + \Delta A, \widehat{\Theta}_1 + \Delta\widehat{\Theta}_1, \widehat{\Theta}_2 + \Delta\widehat{\Theta}_2, \widehat{\Theta}_3 + \Delta\widehat{\Theta}_3$, respectively. These variables correspond to an N number of nodes and each node as an n -dimensional subsystem in the following form

$$\begin{aligned} \dot{x}_i(t) &= (A + \Delta A(t))x_i(t) + \mathcal{G}(\varphi_i(t)) + \sum_{j=1}^N \mathcal{E}_{ij}(\widehat{\Theta}_1 + \Delta\widehat{\Theta}_1(t))x_j(t) + \sum_{j=1}^N \mathcal{H}_{ij}(\widehat{\Theta}_2 + \Delta\widehat{\Theta}_2(t))x_j(t - \alpha(t)) \\ &\quad + \sum_{j=1}^N \mathcal{J}_{ij}(\widehat{\Theta}_3 + \Delta\widehat{\Theta}_3) \int_{t-\delta}^t x_j(s)ds - \mathcal{U}_{iP}\varphi_i(t) - \mathcal{U}_{iI} \int_0^t \varphi_i(s)ds - \mathcal{U}_{iD}\dot{\varphi}_i(t) + \omega_i(t), \end{aligned} \quad (3.20)$$

where $\Delta A(t), \Delta\widehat{\Theta}_1(t), \Delta\widehat{\Theta}_2(t)$ and $\Delta\widehat{\Theta}_3(t)$ are the uncertain time varying matrices with norm bounded and satisfy the following:

$$\begin{bmatrix} \Delta A(t) & \Delta\widehat{\Theta}_1(t) & \Delta\widehat{\Theta}_2(t) & \Delta\widehat{\Theta}_3(t) \end{bmatrix} = \bar{\Upsilon}M(t) \begin{bmatrix} \Pi_1 & \Pi_2 & \Pi_3 & \Pi_4 \end{bmatrix}, \quad (3.21)$$

where, $\bar{\Upsilon}$ and $\Pi_a (a = 1, 2, 3, 4)$ are the known constant matrices, and $M(t)$ is the unknown time-varying matrices with suitable dimension and satisfying the $M^T(t)M(t) \leq I$. Now, the compact form of error system can be given by

$$\dot{\varphi}(t) = (A + \Delta A(t))\varphi(t) + \mathcal{G}(\varphi_i(t)) + (\mathcal{E} \otimes (\widehat{\Theta}_1 + \Delta\widehat{\Theta}_1(t)))\varphi(t) - (\mathcal{H} \otimes (\widehat{\Theta}_2 + \Delta\widehat{\Theta}_2(t)))\varphi(t - \alpha(t))$$

$$+(\mathcal{J} \otimes (\widehat{\Theta}_3 + \Delta\widehat{\Theta}_3(t))) \int_{t-\delta}^t \varphi(s)ds - \mathcal{U}_P\varphi(t) - \mathcal{U}_1 \int_0^t \varphi(s)ds - \mathcal{U}_D\dot{\varphi}(t) + \omega(t). \quad (3.22)$$

Theorem 3.3. For given parameters $\varsigma \leq 1$, ρ , μ , ν and β with known control parameters \mathcal{U}_P , \mathcal{U}_1 and \mathcal{U}_D and the Assumption **H1** being true, the CDNs (3.20) are said to be exponentially stable if there exist positive definite matrices $\mathcal{C}_1, \mathcal{C}_2, \mathcal{C}_3, \mathcal{C}_4, \mathcal{C}_5, \mathcal{B}_1, \mathcal{B}_2$ and $\mathcal{W}_a = \begin{bmatrix} \mathcal{W}_1 & \mathcal{W}_2 \\ \mathbf{\star} & \mathcal{W}_3 \end{bmatrix} > 0$, $\mathcal{W}_b = \begin{bmatrix} \mathcal{W}_4 & \mathcal{W}_5 \\ \mathbf{\star} & \mathcal{W}_6 \end{bmatrix} > 0$ and appropriate dimension matrices \mathcal{N}_r ($r = 1, 2, \dots, 8$) and positive scalars $\lambda_1, \lambda_2, \varepsilon_1$ and ε_2 , such that the following LMIs hold:

$$\widehat{\mathfrak{F}} = \begin{bmatrix} \widehat{\mathfrak{F}} \end{bmatrix}_{13 \times 13} < 0, \quad (3.23)$$

where,

$$\begin{aligned} \widehat{\mathfrak{F}}_{11} &= (\mathcal{B}_1 + \mathcal{B}_1^T) + \mathcal{C}_1 + \mathcal{C}_2 + \mathcal{B}_2 + \varsigma\mathcal{C}_5 + 2\beta\mathcal{B}_1 + 2\beta\mathcal{W}_1 + 2\beta\mathcal{W}_4 + \mathcal{U}_P^T \Xi_1 \mathcal{U}_P + 2 \left[\mathcal{N}_1 A + \mathcal{N}_1 (\mathcal{E} \otimes \widehat{\Theta}_1) - \mathcal{N}_1 \mathcal{U}_P \right] + \\ &\varepsilon_1 \mathcal{U}_P^T \Xi_3 \mathcal{U}_P - \varepsilon_2 \widehat{\Upsilon}_1 + \lambda_1 \Pi_1 \Pi_1^T + \lambda_2 \Pi_2 \Pi_2^T; \widehat{\mathfrak{F}}_{12} = 2\beta\mathcal{W}_2^T + \mathcal{N}_1^T (\mathcal{H} \otimes \widehat{\Theta}_2)^T + \mathcal{N}_2 \left[A + (\mathcal{E} \otimes \widehat{\Theta}_1) - 2\mathcal{U}_P \right] + \lambda_1 \Pi_1 \Pi_3^T; \\ \widehat{\mathfrak{F}}_{13} &= -\mathcal{U}_P^T \mathcal{U}_1 \Xi_1 - \mathcal{N}_1 \mathcal{U}_1 + \mathcal{N}_3 \left[A + (\mathcal{E} \otimes \widehat{\Theta}_1) - \mathcal{U}_P \right] + \varepsilon_1 2\mathcal{U}_P^T \mathcal{U}_1 \Xi_3; \widehat{\mathfrak{F}}_{14} = \mathcal{B}_1 + \mathcal{W}_1^T + \mathcal{W}_4^T + \mathcal{U}_P^T \Xi_1 \mathcal{U}_D - \\ &\left[\mathcal{N}_1 \mathcal{U}_D + \mathcal{N}_1 \right] + \mathcal{N}_4 \left[A + (\mathcal{E} \otimes \widehat{\Theta}_1) - \mathcal{U}_P \right] + 2\varepsilon_1 \mathcal{U}_P^T \Xi_3 \mathcal{U}_D; \widehat{\mathfrak{F}}_{15} = (1 - \varsigma)\mathcal{W}_3 + \mathcal{N}_5 \left[A + (\mathcal{E} \otimes \widehat{\Theta}_1) - \mathcal{U}_P \right]; \\ \widehat{\mathfrak{F}}_{16} &= \mathcal{N}_1 (\mathcal{J} \otimes \widehat{\Theta}_3) + \mathcal{N}_6 \left[A + (\mathcal{E} \otimes \widehat{\Theta}_1) - \mathcal{U}_P \right] + \lambda_1 \Pi_1 \Pi_4^T; \widehat{\mathfrak{F}}_{17} = \mathcal{N}_7 \left[A + (\mathcal{E} \otimes \widehat{\Theta}_1) - \mathcal{U}_P \right] + 2\beta\mathcal{W}_5; \\ \widehat{\mathfrak{F}}_{18} &= \mathcal{W}_5^T + \mathcal{N}_8 \left[A + (\mathcal{E} \otimes \widehat{\Theta}_1) - \mathcal{U}_P \right]; \widehat{\mathfrak{F}}_{19} = \mathcal{N}_1^T; \widehat{\mathfrak{F}}_{110} = \mathcal{N}_1^T - \varepsilon_2 \widehat{\Upsilon}_2; \widehat{\mathfrak{F}}_{112} = \mathcal{N}_1 \overline{\Upsilon}; \widehat{\mathfrak{F}}_{113} = \mathcal{N}_1 \overline{\Upsilon}; \\ \widehat{\mathfrak{F}}_{22} &= -e^{-2\beta\varsigma}(1 - \varsigma)\mathcal{C}_2 + 2\beta\mathcal{W}_3 + \mathcal{N}_2 (\mathcal{H} \otimes \widehat{\Theta}_2) + \lambda_1 \Pi_3 \Pi_3^T; \widehat{\mathfrak{F}}_{23} = \mathcal{N}_2 \mathcal{U}_1 + \mathcal{N}_3 (\mathcal{H} \otimes \widehat{\Theta}_2); \widehat{\mathfrak{F}}_{24} = \\ &\mathcal{W}_2 - \left[\mathcal{N}_2 + \mathcal{N}_2 \mathcal{U}_D \right] + \mathcal{N}_4 (\mathcal{H} \otimes \widehat{\Theta}_2); \widehat{\mathfrak{F}}_{25} = (1 - \varsigma)\mathcal{W}_3 + \mathcal{N}_5 (\mathcal{H} \otimes \widehat{\Theta}_2); \widehat{\mathfrak{F}}_{26} = \mathcal{N}_2 (\mathcal{J} \otimes \widehat{\Theta}_3) + \mathcal{N}_6 \left[\mathcal{H} \otimes \widehat{\Theta}_2 \right]; \\ \widehat{\mathfrak{F}}_{27} &= \mathcal{N}_7 (\mathcal{H} \otimes \widehat{\Theta}_2); \widehat{\mathfrak{F}}_{28} = \mathcal{N}_8 (\mathcal{H} \otimes \widehat{\Theta}_2); \widehat{\mathfrak{F}}_{29} = \mathcal{N}_2^T; \widehat{\mathfrak{F}}_{210} = \mathcal{N}_2^T; \widehat{\mathfrak{F}}_{212} = \mathcal{N}_2 \overline{\Upsilon}; \widehat{\mathfrak{F}}_{213} = \mathcal{N}_2 \overline{\Upsilon}; \widehat{\mathfrak{F}}_{33} = \\ &\mathcal{U}_1^T \Xi_1 \mathcal{U}_1 - 2\mathcal{N}_3 \mathcal{U}_1 + \varepsilon_1 \mathcal{U}_1^T \Xi_3 \mathcal{U}_1; \widehat{\mathfrak{F}}_{34} = \mathcal{U}_1^T \Xi_1 \mathcal{U}_D - \left[\mathcal{N}_3 \mathcal{U}_D + \mathcal{N}_3 \right] + \varepsilon_1 + \mathcal{U}_1^T \Xi_3 \mathcal{U}_D - \mathcal{N}_4 \mathcal{U}_1; \widehat{\mathfrak{F}}_{35} = -\mathcal{N}_5 \mathcal{U}_1; \\ \widehat{\mathfrak{F}}_{36} &= \mathcal{N}_3 \left[\mathcal{J} \otimes \widehat{\Theta}_3 \right] - \mathcal{N}_6 \mathcal{U}_1; \widehat{\mathfrak{F}}_{37} = -\mathcal{N}_7 \mathcal{U}_1; \widehat{\mathfrak{F}}_{38} = -\mathcal{N}_8 \mathcal{U}_1; \widehat{\mathfrak{F}}_{39} = \mathcal{N}_3^T; \widehat{\mathfrak{F}}_{310} = \mathcal{N}_3^T; \widehat{\mathfrak{F}}_{312} = \mathcal{N}_3 \overline{\Upsilon}; \\ \widehat{\mathfrak{F}}_{313} &= \mathcal{N}_3 \overline{\Upsilon}; \widehat{\mathfrak{F}}_{44} = \mathcal{U}_D^T \Xi_1 \mathcal{U}_D + \mathcal{C}_3 + \mathcal{C}_4 - 2 \left[\mathcal{N}_4 \mathcal{U}_D + \mathcal{N}_4 \right] + \varepsilon_1 \mathcal{U}_D^T \Xi_2 \mathcal{U}_D; \widehat{\mathfrak{F}}_{45} = - \left[\mathcal{N}_5 \mathcal{U}_D + \mathcal{N}_5 \right]; \\ \widehat{\mathfrak{F}}_{46} &= \mathcal{N}_4 (\mathcal{J} \otimes \widehat{\Theta}_3) - \left[\mathcal{N}_6 \mathcal{U}_D + \mathcal{N}_6 \right]; \widehat{\mathfrak{F}}_{47} = \mathcal{W}_5^T - \left[\mathcal{N}_7 \mathcal{U}_D + \mathcal{N}_7 \right]; \widehat{\mathfrak{F}}_{48} = \left[\mathcal{N}_8 \mathcal{U}_D + \mathcal{N}_8 \right]; \widehat{\mathfrak{F}}_{49} = \mathcal{N}_4^T; \\ \widehat{\mathfrak{F}}_{410} &= \mathcal{N}_4^T; \widehat{\mathfrak{F}}_{412} = \mathcal{N}_4 \overline{\Upsilon}; \widehat{\mathfrak{F}}_{413} = \mathcal{N}_4 \overline{\Upsilon}; \widehat{\mathfrak{F}}_{55} = -(1 - \varsigma)e^{-2\beta\varsigma}\mathcal{C}_4; \widehat{\mathfrak{F}}_{56} = \mathcal{N}_5 (\mathcal{J} \otimes \widehat{\Theta}_3); \widehat{\mathfrak{F}}_{59} = \mathcal{N}_5^T; \\ \widehat{\mathfrak{F}}_{510} &= \mathcal{N}_5^T; \widehat{\mathfrak{F}}_{512} = \mathcal{N}_5 \overline{\Upsilon}; \widehat{\mathfrak{F}}_{513} = \mathcal{N}_5 \overline{\Upsilon}; \widehat{\mathfrak{F}}_{66} = -\frac{e^{2\beta\varsigma}}{\delta}\mathcal{C}_5 + \mathcal{N}_6 (\mathcal{J} \otimes \widehat{\Theta}_3) + \lambda_1 \Pi_4 \Pi_4^T; \widehat{\mathfrak{F}}_{67} = \mathcal{N}_7 (\mathcal{J} \otimes \widehat{\Theta}_3); \\ \widehat{\mathfrak{F}}_{68} &= \mathcal{N}_8 (\mathcal{J} \otimes \widehat{\Theta}_3); \widehat{\mathfrak{F}}_{69} = \mathcal{N}_6^T; \widehat{\mathfrak{F}}_{610} = \mathcal{N}_6^T; \widehat{\mathfrak{F}}_{612} = \mathcal{N}_6 \overline{\Upsilon}; \widehat{\mathfrak{F}}_{613} = \mathcal{N}_6 \overline{\Upsilon}; \widehat{\mathfrak{F}}_{77} = -e^{-2\beta\varsigma}\mathcal{C}_1 + 2\beta\mathcal{W}_6; \widehat{\mathfrak{F}}_{78} = \\ &\mathcal{W}_5^T; \widehat{\mathfrak{F}}_{79} = \mathcal{N}_7^T; \widehat{\mathfrak{F}}_{710} = \mathcal{N}_7^T; \widehat{\mathfrak{F}}_{712} = \mathcal{N}_7 \overline{\Upsilon}; \widehat{\mathfrak{F}}_{713} = \mathcal{N}_7 \overline{\Upsilon}; \widehat{\mathfrak{F}}_{88} = -e^{-2\beta\varsigma}\mathcal{C}_3; \widehat{\mathfrak{F}}_{89} = \mathcal{N}_8^T; \widehat{\mathfrak{F}}_{810} = \mathcal{N}_8^T; \\ \widehat{\mathfrak{F}}_{812} &= \mathcal{N}_8 \overline{\Upsilon}; \widehat{\mathfrak{F}}_{813} = \mathcal{N}_8 \overline{\Upsilon}; \widehat{\mathfrak{F}}_{99} = -\Xi_1 - \varepsilon_1 I; \widehat{\mathfrak{F}}_{1010} = -\varepsilon_2 I; \widehat{\mathfrak{F}}_{1111} = \text{diag}\left\{ \frac{-\rho_1 + 2\beta + \mu_1}{v_1}, \frac{-\rho_2 + 2\beta + \mu_1}{v_2}, \frac{-\rho_N + 2\beta + \mu_1}{v_N} \right\}; \\ \widehat{\mathfrak{F}}_{1212} &= -\lambda_1 I; \widehat{\mathfrak{F}}_{1313} = -\lambda_2 I. \end{aligned}$$

Proof. Based on the condition in (3.21), we are able to express that the subsequent $A + \Delta A$, $\widehat{\Theta}_1 + \Delta \widehat{\Theta}_1$, $\widehat{\Theta}_2 + \Delta \widehat{\Theta}_2$, and $\widehat{\Theta}_3 + \Delta \widehat{\Theta}_3$ are replaced with $A + \bar{Y}M(t)\Pi_1$, $\Theta_1 + \bar{Y}M(t)\Pi_2$, $\Theta_2 + \bar{Y}M(t)\Pi_3$, $\Theta_3 + \bar{Y}M(t)\Pi_4$, respectively. Then the LMI (3.1) for the uncertain condition is equivalent to the following condition:

$$\mathfrak{J} + \mathcal{F}_1 + \mathcal{F}_2, \quad (3.24)$$

$$\mathcal{F}_1 = \begin{pmatrix} \Pi_1 \\ \Pi_3 \\ 0 \\ 0 \\ 0 \\ \Pi_4 \\ 0 \\ 0 \\ 0 \\ 0 \\ 0 \end{pmatrix} M(t) \begin{pmatrix} \bar{Y}\mathcal{N}_7^T \\ \bar{Y}\mathcal{N}_2^T \\ \bar{Y}\mathcal{N}_3^T \\ \bar{Y}\mathcal{N}_4^T \\ \bar{Y}\mathcal{N}_5^T \\ \bar{Y}\mathcal{N}_6^T \\ \bar{Y}\mathcal{N}_7^T \\ \bar{Y}\mathcal{N}_8^T \\ 0 \\ 0 \\ 0 \end{pmatrix}^T + \begin{pmatrix} \bar{Y}\mathcal{N}_1^T \\ \bar{Y}\mathcal{N}_2^T \\ \bar{Y}\mathcal{N}_3^T \\ \bar{Y}\mathcal{N}_4^T \\ \bar{Y}\mathcal{N}_5^T \\ \bar{Y}\mathcal{N}_6^T \\ \bar{Y}\mathcal{N}_7^T \\ \bar{Y}\mathcal{N}_8^T \\ 0 \\ 0 \\ 0 \end{pmatrix} M^T(t) \begin{pmatrix} \Pi_1 \\ \Pi_3 \\ 0 \\ 0 \\ 0 \\ \Pi_4 \\ 0 \\ 0 \\ 0 \\ 0 \\ 0 \end{pmatrix}^T, \quad (3.25)$$

$$\mathcal{F}_2 = \begin{pmatrix} \Pi_2 \\ 0 \\ 0 \\ 0 \\ 0 \\ 0 \\ 0 \\ 0 \\ 0 \\ 0 \\ 0 \end{pmatrix} M(t) \begin{pmatrix} \bar{Y}\mathcal{N}_1^T \\ \bar{Y}\mathcal{N}_2^T \\ \bar{Y}\mathcal{N}_3^T \\ \bar{Y}\mathcal{N}_4^T \\ \bar{Y}\mathcal{N}_5^T \\ \bar{Y}\mathcal{N}_6^T \\ \bar{Y}\mathcal{N}_7^T \\ \bar{Y}\mathcal{N}_8^T \\ 0 \\ 0 \\ 0 \end{pmatrix}^T + \begin{pmatrix} \bar{Y}\mathcal{N}_1^T \\ \bar{Y}\mathcal{N}_2^T \\ \bar{Y}\mathcal{N}_3^T \\ \bar{Y}\mathcal{N}_4^T \\ \bar{Y}\mathcal{N}_5^T \\ \bar{Y}\mathcal{N}_6^T \\ \bar{Y}\mathcal{N}_7^T \\ \bar{Y}\mathcal{N}_8^T \\ 0 \\ 0 \\ 0 \end{pmatrix} M^T(t) \begin{pmatrix} \Pi_2 \\ 0 \\ 0 \\ 0 \\ 0 \\ 0 \\ 0 \\ 0 \\ 0 \\ 0 \\ 0 \end{pmatrix}^T. \quad (3.26)$$

By Lemma (2.3), necessary and sufficient conditions,

$$\mathcal{F}_1 \leq \lambda_1 \begin{pmatrix} \Pi_1 \\ \Pi_3 \\ 0 \\ 0 \\ 0 \\ \Pi_4 \\ 0 \\ 0 \\ 0 \\ 0 \\ 0 \end{pmatrix} \begin{pmatrix} \Pi_1 \\ \Pi_3 \\ 0 \\ 0 \\ 0 \\ \Pi_4 \\ 0 \\ 0 \\ 0 \\ 0 \\ 0 \end{pmatrix}^T + \lambda_1^{-1} \begin{pmatrix} \bar{Y}\mathcal{N}_7^T \\ \bar{Y}\mathcal{N}_2^T \\ \bar{Y}\mathcal{N}_3^T \\ \bar{Y}\mathcal{N}_4^T \\ \bar{Y}\mathcal{N}_5^T \\ \bar{Y}\mathcal{N}_6^T \\ \bar{Y}\mathcal{N}_7^T \\ \bar{Y}\mathcal{N}_8^T \\ 0 \\ 0 \\ 0 \end{pmatrix} \begin{pmatrix} \bar{Y}\mathcal{N}_1^T \\ \bar{Y}\mathcal{N}_2^T \\ \bar{Y}\mathcal{N}_3^T \\ \bar{Y}\mathcal{N}_4^T \\ \bar{Y}\mathcal{N}_5^T \\ \bar{Y}\mathcal{N}_6^T \\ \bar{Y}\mathcal{N}_7^T \\ \bar{Y}\mathcal{N}_8^T \\ 0 \\ 0 \\ 0 \end{pmatrix}^T,$$

$$\mathcal{F}_2 \leq \lambda_2 \begin{pmatrix} \Pi_2 \\ 0 \\ 0 \\ 0 \\ 0 \\ 0 \\ 0 \\ 0 \\ 0 \\ 0 \\ 0 \end{pmatrix} \begin{pmatrix} \Pi_2 \\ 0 \\ 0 \\ 0 \\ 0 \\ 0 \\ 0 \\ 0 \\ 0 \\ 0 \\ 0 \end{pmatrix}^T + \lambda_2^{-1} \begin{pmatrix} \bar{\Upsilon} \mathcal{N}_1^T \\ \bar{\Upsilon} \mathcal{N}_2^T \\ \bar{\Upsilon} \mathcal{N}_3^T \\ \bar{\Upsilon} \mathcal{N}_4^T \\ \bar{\Upsilon} \mathcal{N}_5^T \\ \bar{\Upsilon} \mathcal{N}_6^T \\ \bar{\Upsilon} \mathcal{N}_7^T \\ \bar{\Upsilon} \mathcal{N}_8^T \\ 0 \\ 0 \\ 0 \end{pmatrix} \begin{pmatrix} \bar{\Upsilon} \mathcal{N}_1^T \\ \bar{\Upsilon} \mathcal{N}_2^T \\ \bar{\Upsilon} \mathcal{N}_3^T \\ \bar{\Upsilon} \mathcal{N}_4^T \\ \bar{\Upsilon} \mathcal{N}_5^T \\ \bar{\Upsilon} \mathcal{N}_6^T \\ \bar{\Upsilon} \mathcal{N}_7^T \\ \bar{\Upsilon} \mathcal{N}_8^T \\ 0 \\ 0 \\ 0 \end{pmatrix}^T,$$

Applying Schur complements, we can obtain from (3.23) that $\widehat{\mathfrak{J}}_1 < 0$. This complete the proof.

Remark 3.4. *This work addresses the exponential synchronization of CDNs with hybrid delays using PID controller, in contrast to some research results on exponential synchronization of CDNs with time-varying delays [24, 54, 57]. In contrast to the approach used in [24, 54, 57], which investigated time scale, sample-data control, and impulsive effects, respectively, we studied PID controller with event-triggered mechanism using LMIs to directly incorporate the system's numerous coupling components in the hypothetical matrix in this paper. In addition, the method in [54] is distinct from applying appropriate Free-weight matrices to solve the problem with (3.1). As a result, the approach presented in this work is more effective while maintaining the system's complexity.*

Remark 3.5. *Compared with [54], which did not take into account the influence of any controls while studying the synchronization of multi-weighted complex dynamical networks, our proposed results can guarantee exponential synchronization for CDNs with hybrid delays and event-triggered mechanisms. Particularly distinct from the standard results of PI/PD controllers in [52] and [53], in this research, we investigate PID controller as well as parameter uncertainties with PID controller, which is distinct from previous studies. In Table 1, a comparison table with previously published results is shown below.*

Table 1. Comparison with other works.

	[10]	[6, 24, 54]	[52]	[53]	Our Paper
CDNs	√	√	√	√	√
Exponential Synchronization	×	√	×	×	√
PI/PD Controller	×	×	√	√	√
PID Controller	×	×	×	√	√
Uncertain terms	×	×	×	×	√

4. Numerical examples

This section aims to illustrate the effectiveness of the main results developed in this paper using two numerical examples adopted from the literature.

Example 4.1. Consider the general complex dynamical networks consisting of 5 nodes and each node as a 2-dimensional subsystem in the following form:

$$\begin{aligned} \dot{x}_i(t) = & \mathcal{A}x_i(t) + \mathcal{G}(\varphi_i(t)) + \sum_{j=1}^5 \mathcal{E}_{ij}\Theta_1x_j(t) + \sum_{j=1}^5 \mathcal{H}_{ij}\Theta_2x_j(t - \alpha(t)) + \sum_{j=1}^5 \mathcal{J}_{ij}\Theta_3 \int_{t-\delta}^t x_j(s)ds \\ & - \mathcal{U}_{iP}\varphi_i(t) - \mathcal{U}_{iI} \int_0^t \varphi_i(s)ds - \mathcal{U}_{iD}\dot{\varphi}_i(t) + \omega_i(t). \end{aligned} \quad (4.1)$$

The state and inner-coupling matrices are constructed as follows:

$$\begin{aligned} \mathcal{A} = & \begin{pmatrix} 3.8 & 3.20 \\ 1.45 & 1.78 \end{pmatrix}, \quad \mathcal{E} = \mathcal{H} = \mathcal{J} = \begin{pmatrix} -3 & 0.5 & -0.1 & 0 & 0 \\ 0.5 & -0.4 & -1 & 0 & 0 \\ 1 & 1.4 & -3 & 0 & 0.2 \\ 0 & 0 & 0 & -1 & 0.6 \\ 0 & 0 & 0 & 0.4 & -2 \end{pmatrix}, \\ \Theta_1 = & \begin{pmatrix} 0.25 & 0 \\ 0 & 0.25 \end{pmatrix}, \quad \Theta_2 = \begin{pmatrix} 0.15 & 0 \\ 0 & 0.15 \end{pmatrix}, \quad \Theta_3 = \begin{pmatrix} 0.35 & 0 \\ 0 & 0.35 \end{pmatrix}. \end{aligned}$$

Also, the nonlinear dynamical function can be chosen as

$$\mathcal{G}(\varphi_i(t)) = \begin{bmatrix} \tanh(0.3^*\varphi_{i1}(t)) \\ \tanh(0.41^*\varphi_{i2}(t)) \end{bmatrix},$$

which satisfies the condition that Υ_1 and Υ_2 can be given by

$$\Upsilon_1 = \begin{pmatrix} -0.6 & -0.3 \\ 0.1 & 0.1 \end{pmatrix}, \quad \Upsilon_2 = \begin{pmatrix} -0.33 & -41 \\ 0.3 & 0.25 \end{pmatrix},$$

since parameter and threshold values can be chosen as $\varsigma = 0.5$, $\beta = 0.02$, $\rho_1 = \rho_2 = \rho_3 = \rho_4 = \rho_5 = 5$ and $\nu_1 = \nu_2 = \nu_3 = \nu_4 = \nu_5 = 4$. Also, $\mu_1 = 0.15$, $\mu_2 = 0.18$, $\mu_3 = 0.16$, $\mu_4 = 0.2$, $\mu_5 = 0.12$ and the upper bound $\alpha = 2.5$. Due to the absence of control strategy in place, the state trajectories of the nodes in delayed CDNs cannot be synchronized with the trajectory of the isolated node. This is primarily because of the coupling effects and time-varying delays that are present. Therefore, we suggest using the PID controller in conjunction with the dynamic event-triggered strategy to synchronize all of the states to the target node. This will allow the complex network that is being considered to reach a state of synchronization. Eventually, to reach an exponential synchronization for delayed CDNs, our plan is to use a proportional control algorithm. According to the first theorem, if we assume that \mathcal{U}_I and \mathcal{U}_D will always remain equal to zero, the delayed complex dynamical network will be able to accomplish exponential synchronization when $\mathcal{U}_P = 25$. The synchronization error trajectories φ_{j1} and φ_{j2} under the proportional controller are depicted in Figures 1 and 2. An illustration of the control input for the delayed CDN can be seen in Figure 3.

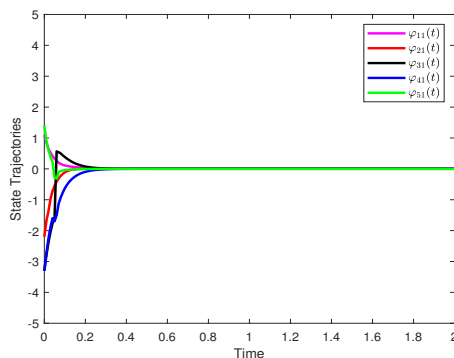


Figure 1. Evolution of synchronization error $\varphi_{j1}(t)$ (Under Proportional controller), ($j = 1, 2, 3, 4, 5$).

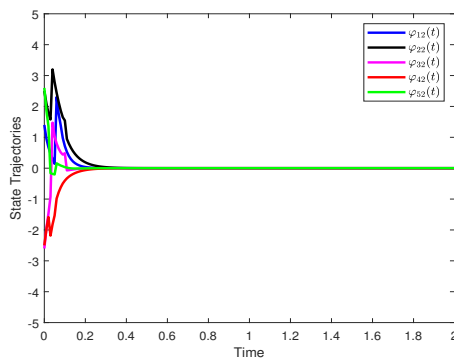


Figure 2. Evolution of synchronization error $\varphi_{j2}(t)$ (Under Proportional controller), ($j = 1, 2, 3, 4, 5$).

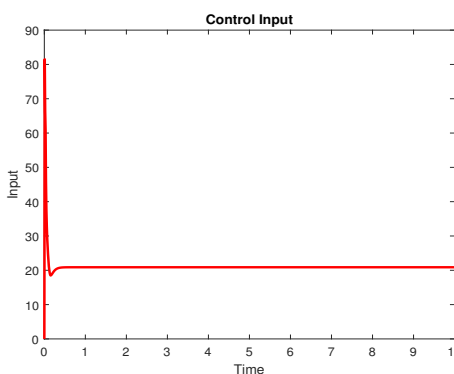


Figure 3. Control input.

Next, if we assume that \mathcal{U}_D will always remain equal to zero, the delayed CDNs will be able to accomplish exponential synchronization when $\mathcal{U}_P = 10$ and $\mathcal{U}_1 = 55$. The synchronization error trajectories φ_{j1} and φ_{j2} under the proportional controller are depicted in Figures 4 and 5. An

illustration of the control input for the delayed CDNs is shown in Figure 6.

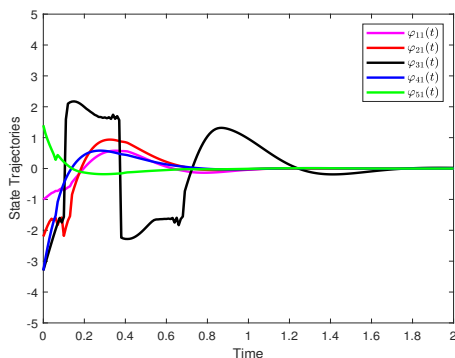


Figure 4. Evolution of synchronization error $\varphi_{j1}(t)$ (Under Proportional Integral controller), $(j = 1, 2, 3, 4, 5)$.

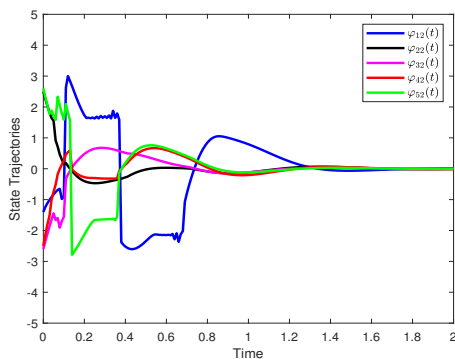


Figure 5. Evolution of synchronization error $\varphi_{j2}(t)$ (Under Proportional Integral controller), $j = 1, 2, 3, 4, 5$.

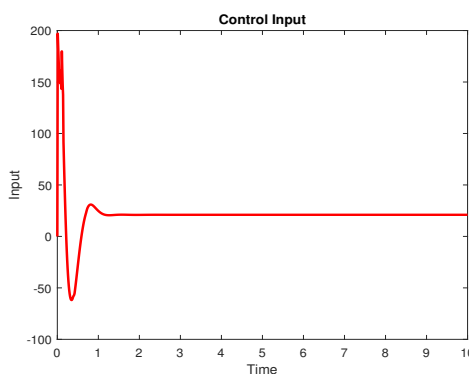


Figure 6. Control input.

Next, if we assume that \mathcal{U}_1 will always remain equal to zero, the delayed complex dynamical network will be able to accomplish exponential synchronization when $\mathcal{U}_P = 40$ and $\mathcal{U}_D = 0.55$. The

synchronization error trajectories φ_{j1} and φ_{j2} under the proportional controller are depicted in Figures 7 and 8. An illustration of the control input for the delayed CDN can be seen in Figure 9.

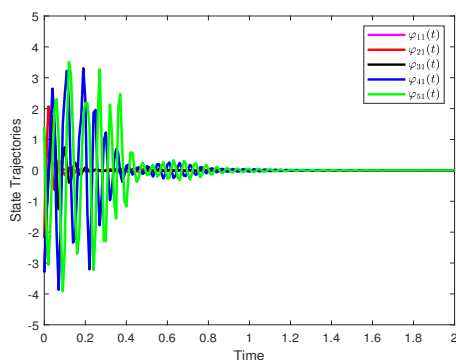


Figure 7. Evolution of synchronization error $\varphi_{j1}(t)$ (Under Proportional Derivative controller), ($j = 1, 2, 3, 4, 5$).

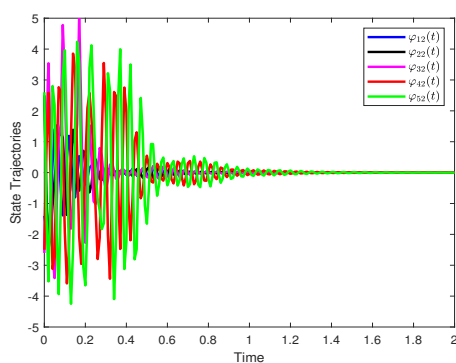


Figure 8. Evolution of synchronization error $\varphi_{j2}(t)$ (Under Proportional Derivative controller), ($j = 1, 2, 3, 4, 5$).

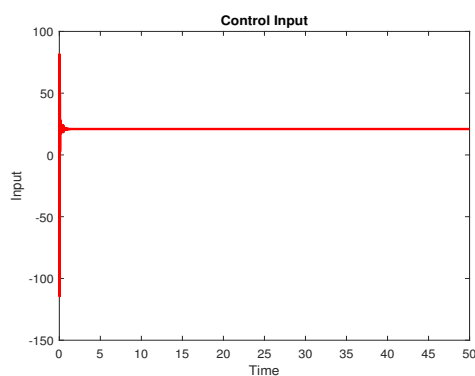


Figure 9. Control input.

Next, the delayed complex dynamical network will be able to accomplish exponential

synchronization using PID controller when $\mathcal{U}_P = 40$, $\mathcal{U}_I = 55$ and $\mathcal{U}_D = 0.65$. The synchronization error trajectories φ_{j1} and φ_{j2} under the proportional controller are depicted in Figures 10 and 11. An illustration of the control input for the delayed CDNs can be seen in Figure 12.

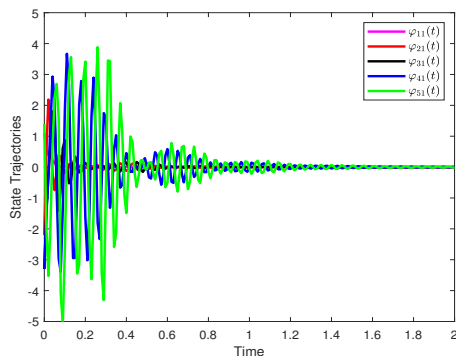


Figure 10. Evolution of synchronization error $\varphi_{j1}(t)$ (Under Proportional Integral Derivative controller), ($j = 1, 2, 3, 4, 5$).

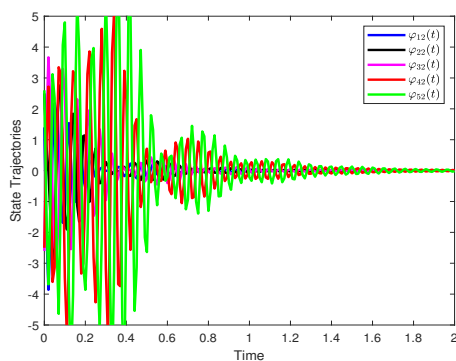


Figure 11. Evolution of synchronization error $\varphi_{j2}(t)$ (Under Proportional Integral Derivative controller), ($j = 1, 2, 3, 4, 5$).

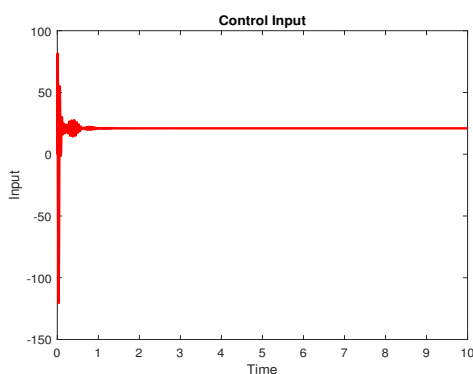


Figure 12. Control input.

By using the MATLAB LMI tool box, we have obtained the scalar values $\varepsilon_1 = 8.6389$, $\varepsilon_2 = 1.0853$, and positive definite matrices are given by

$$\begin{aligned} \mathcal{W}_1 &= \begin{pmatrix} 2.1399 & -0.2508 \\ -0.2508 & 1.6640 \end{pmatrix}, \quad \mathcal{W}_2 = \begin{pmatrix} 1.5791 & -0.3814 \\ -0.3814 & 1.0592 \end{pmatrix}, \quad \mathcal{W}_3 = \begin{pmatrix} 4.9061 & -1.4585 \\ -1.4585 & 4.0388 \end{pmatrix}, \\ \mathcal{W}_4 &= \begin{pmatrix} 2.9941 & 0.2839 \\ 0.2839 & 2.0446 \end{pmatrix}, \quad \mathcal{W}_5 = \begin{pmatrix} 1.7289 & 0.1172 \\ 0.1172 & 0.0866 \end{pmatrix}, \quad \mathcal{W}_6 = \begin{pmatrix} 26.8389 & 0.0048 \\ 0.0048 & -0.0128 \end{pmatrix}, \\ \mathcal{N}_1 &= \begin{pmatrix} 1.1918 & -0.0527 \\ -0.0527 & 0.0065 \end{pmatrix}, \quad \mathcal{N}_2 = \begin{pmatrix} 2.5062 & -0.1357 \\ -0.1357 & 0.0490 \end{pmatrix}, \quad \mathcal{N}_3 = \begin{pmatrix} 7.6356 & -0.2856 \\ -0.2856 & 0.0350 \end{pmatrix}, \\ \mathcal{N}_4 &= \begin{pmatrix} 9.8037 & -0.3312 \\ -0.3312 & 0.0490 \end{pmatrix}, \quad \mathcal{N}_5 = \begin{pmatrix} 4.4903 & 0.0339 \\ 0.0339 & 0.0296 \end{pmatrix}, \quad \mathcal{N}_6 = \begin{pmatrix} 1.2464 & 0.0088 \\ 0.0088 & -0.0001 \end{pmatrix}, \\ \mathcal{N}_7 &= \begin{pmatrix} 3.6973 & 0.0116 \\ 0.0116 & 0.0551 \end{pmatrix}, \quad \mathcal{N}_8 = \begin{pmatrix} 4.5033 & 0.0128 \\ 0.0128 & 0.0746 \end{pmatrix}, \quad \mathcal{E}_1 = \begin{pmatrix} 2.1399 & -0.2508 \\ -0.2508 & 1.6640 \end{pmatrix}, \\ \mathcal{E}_2 &= \begin{pmatrix} 2.0314 - 0.1100 & & \\ & -0.1100 & 1.4816 \end{pmatrix}, \quad \mathcal{E}_3 = \begin{pmatrix} 2.9759 & 0.2172 \\ 0.2172 & 3.2190 \end{pmatrix}, \quad \mathcal{E}_4 = \begin{pmatrix} 1.0735 & 0.1313 \\ 0.1313 & 1.2715 \end{pmatrix}, \\ \mathcal{E}_5 &= \begin{pmatrix} 1.0984 & 0.1347 \\ 0.1347 & 1.3858 \end{pmatrix}, \quad \mathcal{B}_1 = \begin{pmatrix} 0.7948 & 0.2775 \\ 0.2775 & 1.1939 \end{pmatrix}, \quad \mathcal{B}_2 = \begin{pmatrix} 1.7240 & 0.1790 \\ 0.1790 & 1.9329 \end{pmatrix}. \end{aligned}$$

Example 4.2. Consider the general uncertain CDNs consisting of 3 nodes and each node as a 2-dimensional subsystem in the following form:

$$\begin{aligned} \dot{x}_i(t) &= (A + \Delta A(t))x_i(t) + \mathcal{G}(\varphi_i(t)) + \sum_{j=1}^3 \mathcal{E}_{ij}(\widehat{\Theta}_1 + \Delta \widehat{\Theta}_1(t))x_j(t) + \sum_{j=1}^3 \mathcal{H}_{ij}(\widehat{\Theta}_2 + \Delta \widehat{\Theta}_2(t))x_j(t - \alpha(t)) \\ &+ \sum_{j=1}^3 \mathcal{I}_{ij}(\widehat{\Theta}_3 + \Delta \widehat{\Theta}_3) \int_{t-\delta}^t x_j(s)ds - \mathcal{U}_{iP}\varphi_i(t) - \mathcal{U}_{iI} \int_0^t \varphi_i(s)ds - \mathcal{U}_{iD}\dot{\varphi}_i(t) + \omega_i(t). \quad (4.2) \end{aligned}$$

The state and coupling uncertain matrices are constructed as follows:

$$\begin{aligned} A &= \begin{pmatrix} 3.8 & 3.20 \\ 1.45 & 1.78 \end{pmatrix}, \quad \mathcal{E} = \begin{pmatrix} 3 & -1 & -2 \\ -1 & 2 & -1 \\ -2 & -1 & 3 \end{pmatrix}, \quad \mathcal{H} = \begin{pmatrix} 4 & -2 & -2 \\ -2 & -1 & 3 \\ -2 & 3 & -1 \end{pmatrix}, \\ \mathcal{I} &= \begin{pmatrix} -1 & 2 & 1 \\ 0 & -2 & 2 \\ 1 & 2 & -3 \end{pmatrix}, \quad \widehat{\Theta}_1 = \begin{pmatrix} 0.25 & 0 \\ 0 & 0.25 \end{pmatrix}, \quad \widehat{\Theta}_2 = \begin{pmatrix} 0.15 & 0 \\ 0 & 0.15 \end{pmatrix}, \quad \widehat{\Theta}_3 = \begin{pmatrix} 0.35 & 0 \\ 0 & 0.35 \end{pmatrix}, \\ \Pi_1 &= \begin{pmatrix} 2.54 & 3.52 \\ 5.15 & 0.61 \end{pmatrix}, \quad \Pi_2 = \begin{pmatrix} 1.54 & 0.32 \\ 5.15 & 1.61 \end{pmatrix}, \quad \Pi_3 = \begin{pmatrix} 1.54 & 0.32 \\ 0.15 & 0.13 \end{pmatrix}, \quad \Pi_4 = \begin{pmatrix} 1.34 & 0.22 \\ 0.25 & 0.41 \end{pmatrix}. \end{aligned}$$

Also, the nonlinear dynamical function can be chosen as

$$\mathcal{G}(\varphi_i(t)) = \begin{bmatrix} \tanh(0.2^* \varphi_{i1}(t)) \\ \tanh(0.34^* \varphi_{i2}(t)) \end{bmatrix},$$

which satisfies the condition that Υ_1 and Υ_2 can be given by

$$\Upsilon_1 = \begin{pmatrix} -0.54 & -0.74 \\ 0.12 & 0 \end{pmatrix}, \quad \Upsilon_2 = \begin{pmatrix} -0.43 & -45 \\ 0.32 & 0.2 \end{pmatrix}.$$

The selected known parameters are $\varsigma = 0.5$ and $\beta = 0.01$, with the maximum allowable upper bound set at $\alpha = 2.2$. To achieve exponential synchronization for delayed complex dynamical networks under parameter uncertainties, our strategy involves employing a proportional control algorithm. According to the Theorem 3.3, assuming both \mathcal{U}_1 and \mathcal{U}_D are consistently zero, the delayed complex dynamical network can achieve exponential synchronization with $\mathcal{U}_P = 31$.

The synchronization error trajectories, φ_{i1} and φ_{j2} , under the proportional controller are illustrated in Figures 13 and 14. An illustration of the control input for the delayed CDNs can be found in Figure 15.

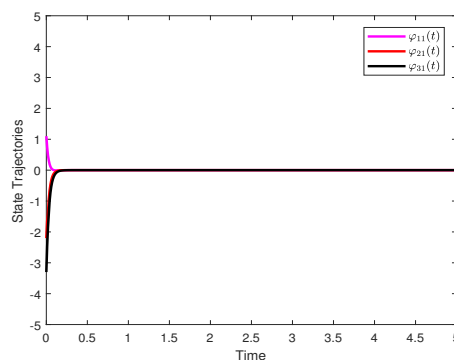


Figure 13. Evolution of synchronization error $\varphi_{j1}(t)$ (Under Proportional controller), $j = 1, 2, 3$.

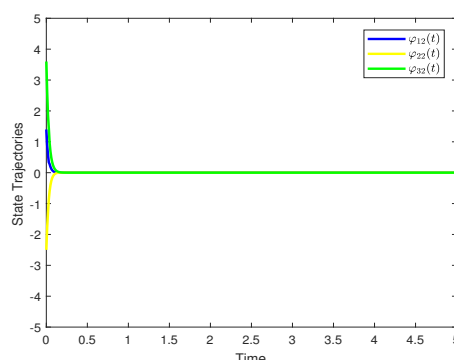


Figure 14. Evolution of synchronization error $\varphi_{j2}(t)$ (Under Proportional controller), $j = 1, 2, 3$.

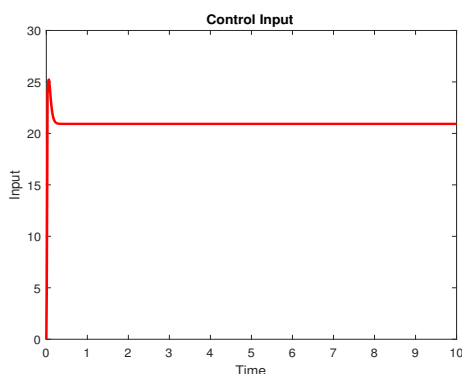


Figure 15. Control input.

Moving forward, applying Theorem 3.3, assuming \mathcal{U}_D remains constantly zero, the delayed CDNs can achieve exponential synchronization with $\mathcal{U}_P = 20$ and $\mathcal{U}_I = 60$. The synchronization error trajectories, φ_{i1} and φ_{j2} , under the proportional controller are depicted in Figures 16 and 17. A visualization of the control input for the delayed CDNs is presented in Figure 18.

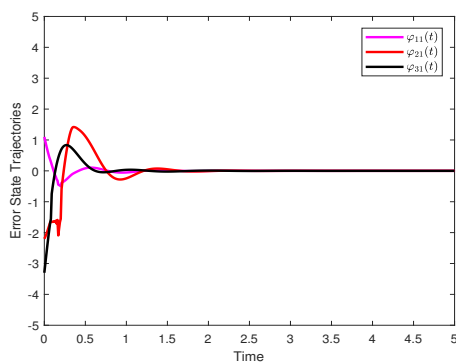


Figure 16. Evolution of synchronization error $\varphi_{ji1}(t)$ (Under Proportional Integral controller), $j = 1, 2, 3$.

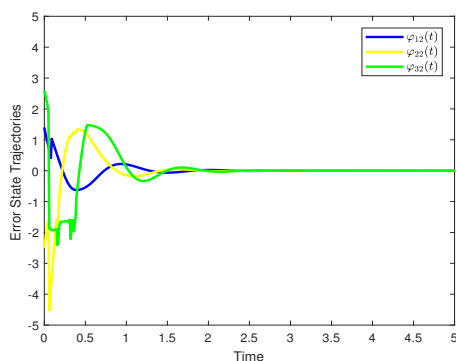


Figure 17. Evolution of synchronization error $\varphi_{j2}(t)$ (Under Proportional Integral controller), $j = 1, 2, 3$.

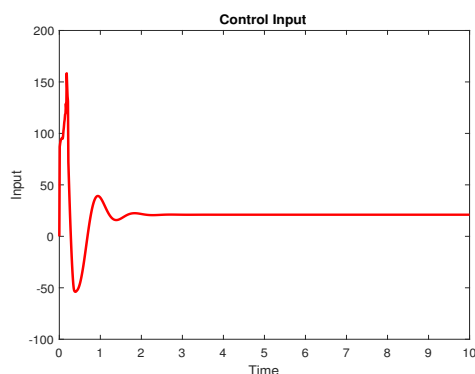


Figure 18. Control input.

Continuing, if we assume \mathcal{U}_1 remains constantly zero, the delayed complex dynamical network can achieve exponential synchronization with $\mathcal{U}_P = 50$ and $\mathcal{U}_D = 0.55$. The synchronization error trajectories, φ_{i1} and φ_{j2} , under the proportional controller are shown in Figures 19 and 20. An illustration of the control input for the delayed CDNs can be seen in Figure 21.

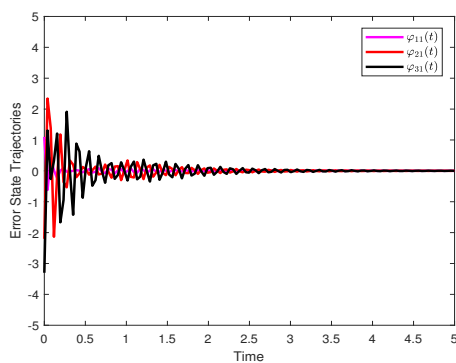


Figure 19. Evolution of synchronization error $\varphi_{j1}(t)$ (Under Proportional Derivative controller), $j = 1, 2, 3$.

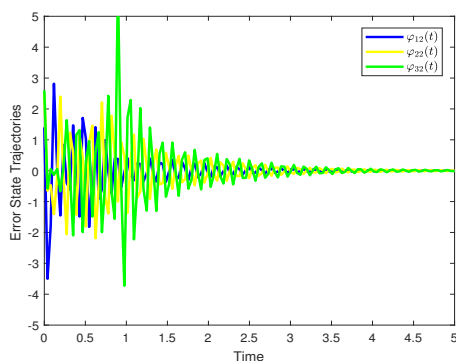


Figure 20. Evolution of synchronization error $\varphi_{j2}(t)$ (Under Proportional Derivative controller), $j = 1, 2, 3$.

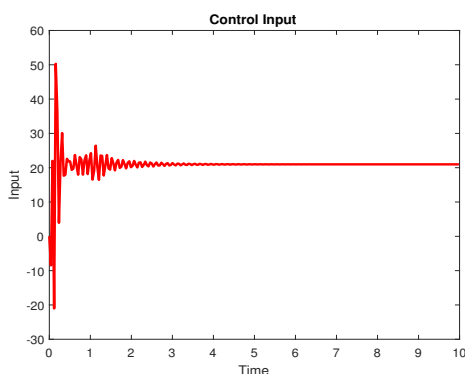


Figure 21. Control input.

Further applying Theorem 3.3, the CDNs can achieve exponential synchronization using a PID controller with $\mathcal{U}_P = 53$, $\mathcal{U}_I = 75$, and $\mathcal{U}_D = 0.65$. The synchronization error trajectories, φ_{j1} and φ_{j2} , under the proportional controller are visualized in Figures 22 and 23. An illustration of the control input for the delayed CDNs is available in Figure 24.

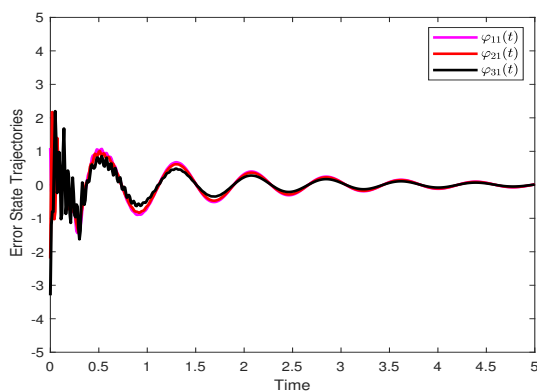


Figure 22. Evolution of synchronization error $\varphi_{j1}(t)$ (Under PID controller), $j = 1, 2, 3$.

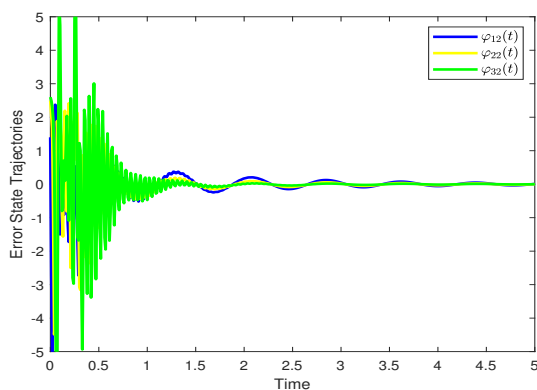


Figure 23. Evolution of synchronization error $\varphi_{j2}(t)$ (Under PID controller), $j = 1, 2, 3$.

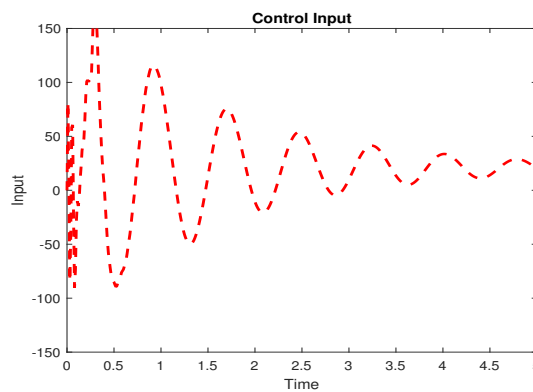


Figure 24. Control input.

By utilizing the MATLAB LMI toolbox, we can get the following scalar values $\varepsilon_1 = 4.5477$, $\varepsilon_2 = 7.0519$ and positive definite matrices:

$$\mathcal{W}_1 = \begin{pmatrix} 2.5546 & -0.0058 \\ -0.0058 & 2.5131 \end{pmatrix}, \quad \mathcal{W}_2 = \begin{pmatrix} 838.5003 & 0.6866 \\ 0.9866 & 847.1332 \end{pmatrix}, \quad \mathcal{W}_3 = \begin{pmatrix} 1.1224 & -0.0069 \\ -0.0069 & 1.0950 \end{pmatrix},$$

$$\mathcal{W}_4 = \begin{pmatrix} 2.9185 & 0.0074 \\ 0.0074 & 2.9413 \end{pmatrix}, \quad \mathcal{W}_5 = \begin{pmatrix} 1.3328 & -0.0144 \\ -0.0144 & 1.3244 \end{pmatrix}, \quad \mathcal{W}_6 = \begin{pmatrix} 362.7104 & 3.6002 \\ 3.6002 & 353.4019 \end{pmatrix},$$

$$\mathcal{N}_1 = \begin{pmatrix} 15.9662 & -0.3751 \\ -0.3751 & 15.5536 \end{pmatrix}, \quad \mathcal{N}_2 = \begin{pmatrix} 17.8032 & -0.4754 \\ -0.4754 & 17.9828 \end{pmatrix}, \quad \mathcal{N}_3 = \begin{pmatrix} 4.5940 & -0.1211 \\ -0.1211 & 4.3925 \end{pmatrix},$$

$$\mathcal{N}_4 = \begin{pmatrix} 10.5927 & -0.1858 \\ -0.1858 & 10.7247 \end{pmatrix}, \quad \mathcal{N}_5 = \begin{pmatrix} 9.8368 & -0.2625 \\ -0.0625 & 9.6927 \end{pmatrix}, \quad \mathcal{N}_6 = \begin{pmatrix} 1.6559 & -0.0148 \\ -0.0148 & 1.5761 \end{pmatrix},$$

$$\mathcal{N}_7 = \begin{pmatrix} 14.2600 & -0.3720 \\ -0.3720 & 14.2429 \end{pmatrix}, \quad \mathcal{N}_8 = \begin{pmatrix} 18.5753 & -0.3917 \\ -0.3917 & 18.5580 \end{pmatrix}, \quad \mathcal{E}_1 = \begin{pmatrix} 1.7252 & 0.1201 \\ 0.0120 & 2.1247 \end{pmatrix},$$

$$\mathcal{E}_2 = \begin{pmatrix} 1.1020 & -0.0023 \\ -0.0023 & 1.1232 \end{pmatrix}, \quad \mathcal{E}_3 = \begin{pmatrix} 1.5381 & -0.0077 \\ -0.0077 & 1.5649 \end{pmatrix}, \quad \mathcal{E}_4 = \begin{pmatrix} 2.1049 & -0.0206 \\ -0.0206 & 1.5649 \end{pmatrix},$$

$$\mathcal{E}_5 = \begin{pmatrix} 9.2451 & -0.0344 \\ -0.0344 & 9.2441 \end{pmatrix}, \quad \mathcal{B}_1 = \begin{pmatrix} 2.4181 & 0.4222 \\ 0.4222 & 2.9580 \end{pmatrix}, \quad \mathcal{B}_2 = \begin{pmatrix} 1.3451 & 0.3942 \\ 0.3942 & 1.6548 \end{pmatrix}.$$

Example 4.3. Consider the complex dynamical networks (4.1) consisting of 8 nodes and each node as a 3-dimensional subsystem, and the known parameters are given as follows:

$$\mathcal{A} = \begin{pmatrix} -1 & 0 & 0 \\ 0 & -1 & 0 \\ 0 & 0 & -1 \end{pmatrix}, \quad \mathcal{E} = \mathcal{H} = \mathcal{J} = \begin{pmatrix} -2 & 0 & 1 & 1 & 0 & 0 & 0 & 0 \\ 0 & -3 & 1 & 1 & 0 & 1 & 0 & 0 \\ 1 & 2 & -3 & 0 & 0 & 0 & 0 & 1 \\ 1 & 1 & 0 & -4 & 1 & 0 & 0 & 1 \\ 0 & 0 & 0 & 1 & -2 & 0 & 1 & 0 \\ 0 & 1 & 0 & 0 & 0 & -2 & 0 & 1 \\ 0 & 0 & 0 & 0 & 1 & 0 & -2 & 1 \\ 0 & 0 & 1 & 1 & 0 & 1 & 1 & -4 \end{pmatrix},$$

$$\Theta_1 = \begin{pmatrix} 0.08 & 0 & 0 \\ 0 & 0.08 & 0 \\ 0 & 0 & 0.08 \end{pmatrix}, \quad \Theta_2 = \begin{pmatrix} 0.1 & 0 & 0 \\ 0 & 0.1 & 0 \\ 0 & 0 & 0.1 \end{pmatrix}, \quad \Theta_3 = \begin{pmatrix} 0.5 & 0 & 0 \\ 0 & 0.5 & 0 \\ 0 & 0 & 0.5 \end{pmatrix}.$$

The nonlinear function is considered as follows:

$$\mathcal{G}(\varphi_i(t)) = \begin{bmatrix} \tanh(0.1^* \varphi_{i1}(t)) \\ \tanh(0.15^* \varphi_{i2}(t)) \\ \tanh(0.2^* \varphi_{i2}(t)) \end{bmatrix}.$$

The parameters and threshold values can be set as follows: $\zeta = 0.2$, $\beta = 0.01$, $\rho_1 = \rho_2 = \rho_3 = \rho_4 = \rho_5 = \rho_6 = \rho_7 = \rho_8 = 2$, and $v_1 = v_2 = v_3 = v_4 = v_5 = v_6 = v_7 = v_8 = 2$. Additionally, $\mu_1 = 0.03$, $\mu_2 = 0.06$, $\mu_3 = 0.02$, $\mu_4 = 0.02$, $\mu_5 = 0.1$, and the upper bound $\alpha = 1.5$. Using the same control parameters from Example 3.1, it can be verified through the Matlab toolbox that inequality (3.1) in Theorem 3.1 is satisfied. The results are shown in Figure 25.

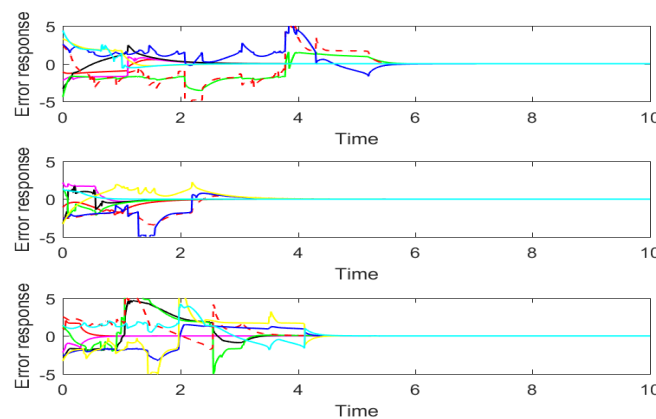


Figure 25. Synchronization of $\varphi_{j1}(t)$, $\varphi_{j2}(t)$, $\varphi_{j3}(t)$ (Under PID controller), ($1 \leq j \leq 8$).

5. Conclusions

In this manuscript, we have presented a novel approach to achieving exponential synchronization in CDNs with hybrid delays by combining PID control with a dynamic event-trigger mechanism. We formulate a comprehensive mathematical model for the network and establish synchronization criteria using LMI techniques. We have also demonstrated the stability of the system under the proposed control approach using Lyapunov stability theory techniques. Our numerical simulations have shown that the proposed approach is effective in achieving exponential synchronization in CDNs with hybrid delays and that the use of PID control parameter values and a dynamic event trigger mechanism can lead to significant improvements in the efficiency and robustness of the control strategy. Our results have important implications for the development of more advanced and effective control strategies for complex systems, particularly in the presence of delays and other sources of uncertainty. We hope that our research will inspire further investigations into the use of PID control and dynamic event trigger mechanisms in CDNs and contribute to the development of more efficient and robust control strategies for complex systems in the future.

Use of AI tools declaration

The authors declare they have not used Artificial Intelligence (AI) tools in the creation of this article.

Acknowledgments

M. Rhaima was supported by Researchers Supporting Project number (RSPD2023R683), King Saud University, Riyadh, Saudi Arabia. The first author gratefully acknowledges that this work is funded by the Centre for Nonlinear Systems, Chennai Institute of Technology (CIT), India, funding number CIT/CNS/2023/RP-005.

Conflict of interest

The author declares that there is no conflict of interest regarding the publication of this paper.

References

1. Y. Yu, Z. Zhang, M. Zhong, Z. Wang, Pinning synchronization and adaptive synchronization of complex-valued inertial neural networks with time-varying delays in fixed-time interval, *J. Franklin I.*, **359** (2022), 1434–1456. <https://doi.org/10.1016/j.jfranklin.2021.11.036>
2. H. Zhao, L. Li, H. Peng, J. Xiao, Y. Yang, M. Zheng, Impulsive control for synchronization and parameters identification of uncertain multi-links complex network, *Nonlinear Dyn.*, **83** (2016), 1437–1451. <https://doi.org/10.1007/S11071-015-2416-3>
3. W. Yu, G. Chen, J. Lü, On pinning synchronization of complex dynamical networks, *Automatica*, **45** (2009), 429–435. <https://doi.org/10.1016/j.automatica.2008.07.016>
4. H. Liu, J. A. Lu, J. Lü, D. J. Hill, Structure identification of uncertain general complex dynamical networks with time delay, *Automatica*, **45** (2009), 1799–1807. <https://doi.org/10.1016/j.automatica.2009.03.022>
5. H. Ren, F. Deng, Y. Peng, Finite time synchronization of markovian jumping stochastic complex dynamical systems with mix delays via hybrid control strategy, *Neurocomputing*, **272** (2018), 683–693. <https://doi.org/10.1016/j.neucom.2017.08.013>
6. Z. H. Guan, Z. W. Liu, G. Feng, Y. W. Wang, Synchronization of complex dynamical networks with time-varying delays via impulsive distributed control, *IEEE T. Circuits-I*, **57** (2010), 2182–2195. <https://doi.org/10.1109/TCSI.2009.2037848>
7. L. Xiao, B. Liao, S. Li, Z. Zhang, L. Ding, L. Jin, Design and analysis of ftznn applied to the real-time solution of a nonstationary lyapunov equation and tracking control of a wheeled mobile manipulator, *IEEE T. Ind. Inform.*, **14** (2018), 98–105. <https://doi.org/10.1109/TII.2017.2717020>
8. L. Xiao, J. Dai, L. Jin, W. Li, S. Li, J. Hou, A noise-enduring and finite-time zeroing neural network for equality-constrained time-varying nonlinear optimization, *IEEE T. Syst. Man Cy.-S.*, **51** (2021), 4729–4740. <https://doi.org/10.1109/TSMC.2019.2944152>
9. J. Zhou, D. Xu, W. Tai, C. K. Ahn, Switched event-triggered H_∞ security control for networked systems vulnerable to aperiodic dos attacks, *IEEE T. Netw. Sci. Eng.*, **10** (2023), 2109–2123. <https://doi.org/10.1109/TNSE.2023.3243095>

10. J. L. Wang, P. C. Wei, H. N. Wu, T. Huang, M. Xu, Pinning synchronization of complex dynamical networks with multiweights, *IEEE T. Syst. Man Cy.-S.*, **49** (2019), 1357–1370. <https://doi.org/10.1109/TSMC.2017.2754466>
11. Q. Li, B. Shen, Z. Wang, T. Huang, J. Luo, Synchronization control for a class of discrete time-delay complex dynamical networks: A dynamic event-triggered approach, *IEEE T. Cybernetics*, **49** (2019), 1979–1986. <https://doi.org/10.1109/TCYB.2018.2818941>
12. X. Yang, J. Lam, D. W. C. Ho, Z. Feng, Fixed-time synchronization of complex networks with impulsive effects via nonchattering control, *IEEE T. Automat. Contr.*, **62** (2017), 5511–5521. <https://doi.org/10.1109/TAC.2017.2691303>
13. H. Shen, X. Hu, X. Wu, S. He, J. Wang, Generalized dissipative state estimation of singularly perturbed switched complex dynamic networks with persistent dwell-time mechanism, *IEEE T. Syst. Man Cy.-S.*, **52** (2020), 1795–1806. <https://doi.org/10.1109/TSMC.2020.3034635>
14. M. S. Raunak, L. J. Osterweil, Resource management for complex, dynamic environments, *IEEE T. Software Eng.*, **39** (2012), 384–402. <https://doi.org/10.1109/TSE.2012.31>
15. L. Wang, H. P. Dai, H. Dong, Y. Y. Cao, Y. X. Sun, Adaptive synchronization of weighted complex dynamical networks through pinning, *Eur. Phys. J. B*, **61** (2008), 335–342. <https://doi.org/10.1140/epjb/e2008-00081-5>
16. J. Yogambigai, M. S. Ali, H. Alsulami, M. S. Alhodaly, Impulsive and pinning control synchronization of markovian jumping complex dynamical networks with hybrid coupling and additive interval time-varying delays, *Commun. Nonlinear Sci.*, **85** (2020), 105215. <https://doi.org/10.1016/j.cnsns.2020.105215>
17. M. S. Anwar, S. Kundu, D. Ghosh, Enhancing synchrony in asymmetrically weighted multiplex networks, *Chaos Soliton. Fract.*, **142** (2021), 110476. <https://doi.org/10.1016/j.chaos.2020.110476>
18. M. S. Anwar, D. Ghosh, N. Frolov, Relay synchronization in a weighted triplex network, *Mathematics*, **9** (2021), 2135. <https://doi.org/10.3390/math9172135>
19. L. V. Gambuzza, M. Frasca, E. Estrada, Hubs-attracting laplacian and related synchronization on networks, *SIAM J. Appl. Dyn. Syst.*, **19** (2020), 1057–1079. <https://doi.org/10.1137/19M1287663>
20. Y. A. Liu, J. Xia, B. Meng, X. Song, H. Shen, Extended dissipative synchronization for semi-markov jump complex dynamic networks via memory sampled-data control scheme, *J. Franklin I.*, **357** (2020), 10900–10920. <https://doi.org/10.1016/j.jfranklin.2020.08.023>
21. Y. Wang, S. Ding, R. Li, Master-slave synchronization of neural networks via event-triggered dynamic controller, *Neurocomputing*, **419** (2021), 215–223. <https://doi.org/10.1016/j.neucom.2020.08.062>
22. Q. Jia, E. S. Mwanandiye, W. K. Tang, Master-slave synchronization of delayed neural networks with time-varying control, *IEEE T. Neur. Net. Lear.*, **32** (2021), 2292–2298. <https://doi.org/10.1109/TNNLS.2020.2996224>
23. C. Hu, H. He, H. Jiang, Fixed/preassigned-time synchronization of complex networks via improving fixed-time stability, *IEEE T. Cybernetics*, **51** (2021), 2882–2892. <https://doi.org/10.1109/TCYB.2020.2977934>

24. J. Zhang, J. Sun, Exponential synchronization of complex networks with continuous dynamics and boolean mechanism, *Neurocomputing*, **307** (2018), 146–152. <https://doi.org/10.1016/j.neucom.2018.03.061>
25. A. Z. Dragicevic, A. Gurtoo, Stochastic control of ecological networks, *J. Math. Biol.*, **85** (2022), 7. <https://doi.org/10.1007/s00285-022-01777-5>
26. J. L. Wang, H. N. Wu, T. Huang, S. Y. Ren, Analysis and pinning control for output synchronization and h_∞ output synchronization of multi-weighted complex networks, In: *Analysis and control of output synchronization for complex dynamical networks*, Singapore: Springer, 2019, 175–205. https://doi.org/10.1007/978-981-13-1352-3_9
27. D. Wang, W. W. Che, H. Yu, J. Y. Li, Adaptive pinning synchronization of complex networks with negative weights and its application in traffic road network, *Int. J. Control Autom. Syst.*, **16** (2018), 782–790. <https://doi.org/10.1007/s12555-017-0161-8>
28. E. Kyriakakis, J. Sparsø, P. Puschner, M. Schoeberl, Synchronizing real-time tasks in time-triggered networks, In: *2021 IEEE 24th international symposium on real-time distributed computing (ISORC)*, 2021, 11–19. <https://doi.org/10.1109/ISORC52013.2021.00013>
29. T. Hu, Z. He, X. Zhang, S. Zhong, K. Shi, Y. Zhang, Adaptive fuzzy control for quasi-synchronization of uncertain complex dynamical networks with time-varying topology via event-triggered communication strategy, *Inform. Sci.*, **582** (2022), 704–724. <https://doi.org/10.1016/j.ins.2021.10.036>
30. K. Krüger, G. Fohler, M. Völp, P. Esteves-Verissimo, Improving security for time-triggered real-time systems with task replication, In: *2018 IEEE 24th international conference on embedded and real-time computing systems and applications (RTCSA)*, 2018, 232–233. <https://doi.org/10.1109/RTCSA.2018.00036>
31. Q. Wang, B. Fu, C. Lin, P. Li, Exponential synchronization of chaotic lur'e systems with time-triggered intermittent control, *Commun. Nonlinear Sci.*, **109** (2022), 106298. <https://doi.org/10.1016/j.cnsns.2022.106298>
32. S. Ding, Z. Wang, Event-triggered synchronization of discrete-time neural networks: A switching approach, *Neural Networks*, **125** (2020), 31–40. <https://doi.org/10.1016/j.neunet.2020.01.024>
33. Y. Li, F. Song, J. Liu, X. Xie, E. Tian, Decentralized event-triggered synchronization control for complex networks with nonperiodic dos attacks, *Int. J. Robust Nonlin.*, **32** (2022), 1633–1653. <https://doi.org/10.1002/rnc.5899>
34. R. Pan, Y. Tan, D. Du, S. Fei, Adaptive event-triggered synchronization control for complex networks with quantization and cyber-attacks, *Neurocomputing*, **382** (2020), 249–258. <https://doi.org/10.1016/j.neucom.2019.11.096>
35. W. Xing, P. Shi, R. K. Agarwal, L. Li, Robust H_∞ pinning synchronization for complex networks with event-triggered communication scheme, *IEEE T. Circuits Syst.-I*, **67** (2020), 5233–5245. <https://doi.org/10.1109/TCSI.2020.3004170>
36. B. Li, Z. Wang, L. Ma, An event-triggered pinning control approach to synchronization of discrete-time stochastic complex dynamical networks, *IEEE T. Neur. Net. Lear.*, **29** (2018), 5812–5822. <https://doi.org/10.1109/TNNLS.2018.2812098>

37. Y. Luo, Y. Yao, Z. Cheng, X. Xiao, H. Liu, Event-triggered control for coupled reaction–diffusion complex network systems with finite-time synchronization, *Physica A*, **562** (2021), 125219. <https://doi.org/10.1016/j.physa.2020.125219>
38. X. Lv, J. Cao, X. Li, M. Abdel-Aty, U. A. Al-Juboori, Synchronization analysis for complex dynamical networks with coupling delay via event-triggered delayed impulsive control, *IEEE T. Cybernetics*, **51** (2021), 5269–5278. <https://doi.org/10.1109/TCYB.2020.2974315>
39. C. X. Shi, G. H. Yang, X. J. Li, Event-triggered output feedback synchronization control of complex dynamical networks, *Neurocomputing*, **275** (2018), 29–39. <https://doi.org/10.1016/j.neucom.2017.05.014>
40. X. Li, H. Wu, J. Cao, A new prescribed-time stability theorem for impulsive piecewise-smooth systems and its application to synchronization in networks, *Appl. Math. Model.*, **115** (2023), 385–397. <https://doi.org/10.1016/j.apm.2022.10.051>
41. X. Li, H. Wu, J. Cao, Prescribed-time synchronization in networks of piecewise smooth systems via a nonlinear dynamic event-triggered control strategy, *Math. Comput. Simulat.*, **203** (2023), 647–668. <https://doi.org/10.1016/j.matcom.2022.07.010>
42. B. Zhou, X. Liao, T. Huang, G. Chen, Pinning exponential synchronization of complex networks via event-triggered communication with combinational measurements, *Neurocomputing*, **157** (2015), 199–207. <https://doi.org/10.1016/j.neucom.2015.01.018>
43. D. Liu, G. H. Yang, Event-triggered synchronization control for complex networks with actuator saturation, *Neurocomputing*, **275** (2018), 2209–2216. <https://doi.org/10.1016/j.neucom.2017.10.054>
44. J. Liu, H. Wu, J. Cao, Event-triggered synchronization in fixed time for semi-markov switching dynamical complex networks with multiple weights and discontinuous nonlinearity, *Commun. Nonlinear Sci.*, **90** (2020), 105400. <https://doi.org/10.1016/j.cnsns.2020.105400>
45. X. Song, R. Zhang, C. K. Ahn, S. Song, Dissipative synchronization of semi-markov jump complex dynamical networks via adaptive event-triggered sampling control scheme, *IEEE Syst. J.*, **16** (2022), 4653–4663. <https://doi.org/10.1109/JSYST.2021.3124082>
46. Q. Dong, P. Yu, Y. Ma, Event-triggered synchronization control of complex networks with adaptive coupling strength, *J. Franklin I.*, **359** (2022), 1215–1234. <https://doi.org/10.1016/j.jfranklin.2021.11.007>
47. H. Lu, Y. Hu, C. Guo, W. Zhou, Cluster synchronization for a class of complex dynamical network system with randomly occurring coupling delays via an improved event-triggered pinning control approach, *J. Franklin I.*, **357** (2020), 2167–2184. <https://doi.org/10.1016/j.jfranklin.2019.11.076>
48. S. Wang, Y. Cao, T. Huang, Y. Chen, S. Wen, Event-triggered distributed control for synchronization of multiple memristive neural networks under cyber-physical attacks, *Inform. Sci.*, **518** (2020), 361–375. <https://doi.org/10.1016/j.ins.2020.01.022>
49. W. Wu, L. He, J. Zhou, Z. Xuan, S. Arik, Disturbance-term-based switching event-triggered synchronization control of chaotic lurie systems subject to a joint performance guarantee, *Commun. Nonlinear Sci.*, **115** (2022), 106774. <https://doi.org/10.1016/j.cnsns.2022.106774>

50. Y. Ni, Z. Wang, Y. Fan, X. Huang, H. Shen, Memory-based event-triggered control for global synchronization of chaotic lur'e systems and its application, *IEEE T. Syst. Man Cy.-S.*, **53** (2023), 1920–1931. <https://doi.org/10.1109/TSMC.2022.3207353>
51. H. Zhang, J. Liu, Event-triggered fuzzy flight control of a two-degree-of-freedom helicopter system, *IEEE T. Fuzzy Syst.*, **29** (2021), 2949–2962. <https://doi.org/10.1109/TFUZZ.2020.3009755>
52. P. Liu, H. Gu, Y. Kang, J. Lü, Global synchronization under PI/PD controllers in general complex networks with time-delay, *Neurocomputing*, **366** (2019), 12–22. <https://doi.org/10.1016/j.neucom.2019.07.028>
53. H. Gu, P. Liu, J. Lü, Z. Lin, PID control for synchronization of complex dynamical networks with directed topologies, *IEEE T. Cybernetics*, **51** (2021), 1334–1346. <https://doi.org/10.1109/tcyb.2019.2902810>
54. S. Aadhithyan, R. Raja, Q. Zhu, J. Alzabut, M. Niezabitowski, C. P. Lim, Exponential synchronization of nonlinear multi-weighted complex dynamic networks with hybrid time varying delays, *Neural Process. Lett.*, **53** (2021), 1035–1063. <https://doi.org/10.1007/s11063-021-10428-7>
55. J. Suo, M. Shi, Y. Li, Y. Yang, Proportional-integral control for synchronization of complex dynamical networks under dynamic event-triggered mechanism, *J. Franklin I.*, **360** (2023), 1436–1453. <https://doi.org/10.1016/j.jfranklin.2022.09.048>
56. S. Boyd, L. El Ghaoui, E. Feron, V. Balakrishnan, *Linear matrix inequalities in system and control theory*, SIAM, 1994.
57. H. Liu, T. Wang, Exponential synchronization of complex dynamical networks via a novel sampled-data control, *Complexity*, **2022** (2022), 2786011. <https://doi.org/10.1155/2022/2786011>
58. Y. He, M. Wu, J. H. She, Delay-dependent exponential stability of delayed neural networks with time-varying delay, *IEEE T. Circuits-II*, **53** (2006), 553–557. <https://doi.org/10.1109/TCSII.2006.876385>



AIMS Press

©2023 the Author(s), licensee AIMS Press. This is an open access article distributed under the terms of the Creative Commons Attribution License (<http://creativecommons.org/licenses/by/4.0>)